Variational Learning is Effective for Large Deep Networks

Yuesong Shen [*1] **Nico Daheim** [*2] **Bai Cong** [3] **Peter Nickl** [4] **Gian Maria Marconi** [4] **Clement Bazan** [3] **Rio Yokota** [3] **Iryna Gurevych** [2] **Daniel Cremers** [1] **Mohammad Emtiyaz Khan** [4] **Thomas Möllenhoff** [4]

Abstract

We give extensive empirical evidence against the common belief that variational learning is ineffective for large neural networks. We show that an optimizer called Improved Variational Online Newton (IVON) consistently matches or outperforms Adam for training large networks such as GPT-2 and ResNets from scratch. IVON's computational costs are nearly identical to Adam but its predictive uncertainty is better. We show several new use cases of IVON where we improve finetuning and model merging in Large Language Models, accurately predict generalization error, and faithfully estimate sensitivity to data. We find overwhelming evidence that variational learning is effective. Code is available at https://github.com/team-approx-bayes/ivon.

1. Introduction

Variational learning can potentially improve many aspects of deep learning, but there remain doubts about its effectiveness for large-scale problems. Popular strategies (Graves, 2011; Blundell et al., 2015) do not easily perform well, even on moderately-sized problems, which has led some to believe that it is impossible to get both good accuracy and uncertainty (Trippe & Turner, 2017; Foong et al., 2020; Coker et al., 2022). Variational methods generally have higher costs or tricky implementations (Kingma et al., 2015; Hernández-Lobato & Adams, 2015; Zhang et al., 2018; Khan et al., 2018; Osawa et al., 2019), and they struggle to keep up with the ever-increasing scale of deep learning.

Currently, no variational method can accurately train Large Language Models (LLMs) from scratch at a cost, say, similar to Adam (Kingma & Ba, 2015). This is excluding methods such as MC-dropout (Gal & Ghahramani, 2016), stochastic weight averaging (SWAG) (Maddox et al., 2019), and Laplace (MacKay, 1992), which do not directly optimize the variational objective, even though they have variational interpretations. Ideally, we want a direct optimization of the objective to match Adam's accuracy without increasing the cost, and also yield good weight-uncertainty to improve calibration, model averaging, knowledge transfer, etc.

In this paper, we present the Improved Variational Online Newton (IVON) method, which adapts the method of Lin et al. (2020) to large scale and obtains state-of-the-art accuracy and uncertainty at nearly identical cost as Adam. Fig. 1 shows some examples where, for training GPT-2 (773M parameters) from scratch, IVON gives 0.4 reduction in validation perplexity over AdamW and, for ResNet-50 (25.6M parameters) on ImageNet, it gives around 2% more accurate predictions that are also better calibrated. For image classification, we never observe severe overfitting like AdamW and consistently obtain better or comparable results to SGD.

We introduce practical tricks necessary to achieve good performance and present an Adam-like implementation (Alg. 1) which uses a simplified Hessian-estimation scheme to both adapt the learning rate and estimate weight-uncertainty. This also makes IVON a unique second-order optimizer that consistently performs better than Adam at a similar cost. We present extensive numerical experiments and new use cases to demonstrate its effectiveness. We find that,

1. IVON gets better or comparable predictive uncertainty to alternatives, such as, MC-dropout and SWAG.
2. It works well for finetuning LLMs and reduces the cost of model-merging.
3. It can be used to faithfully predict generalization which is useful for diagnostics and early stopping.
4. It is useful to understand sensitivity to data which is often challenging at large-scale due to ill-conditioning.

Overall, we find overwhelming evidence that variational learning is not only effective but also useful for large deep networks, especially LLMs. IVON is easily amenable to flexible posterior forms (Lin et al., 2019), and we expect it to help researchers further investigate the benefits of Bayesian principles to improve deep learning.

[*]Equal contribution [1]Technical University of Munich & Munich Center for Machine Learning, Munich, Germany [2]UKP Lab, Technical University of Darmstadt & hessian.AI, Darmstadt, Germany [3]Tokyo Institute of Technology, Tokyo, Japan [4]RIKEN Center for AI Project, Tokyo, Japan. Correspondence to: Thomas Möllenhoff <thomas.moellenhoff@riken.jp>.

Proceedings of the 41st International Conference on Machine Learning, Vienna, Austria. PMLR 235, 2024. Copyright 2024 by the author(s).

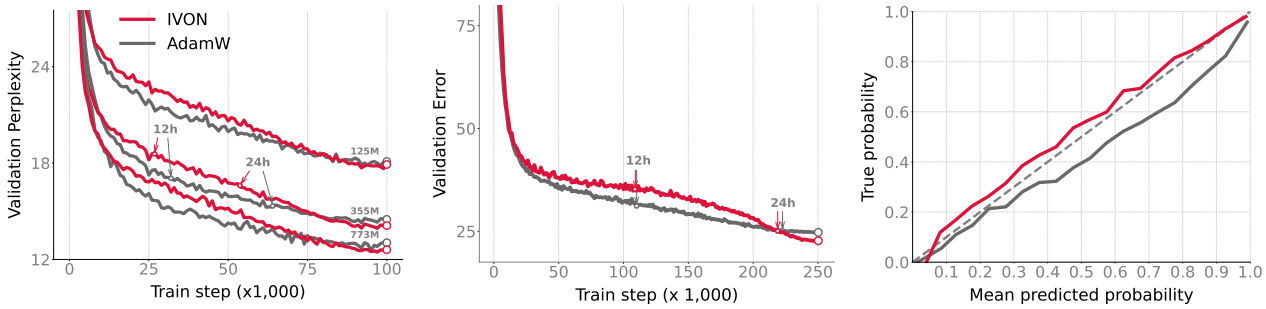

(a) GPT-2 on OpenWebText (b) ResNet-50 on ImageNet (c) Calibration on ImageNet

Figure 1: First two panels show that IVON closely matches the trajectory of AdamW (Loshchilov & Hutter, 2017) for training GPT-2 on OpenWebText and ResNet-50 on ImageNet. The computational costs of IVON and AdamW are nearly identical. Runtime in hours (h) is indicated by the arrows. The third panel shows that the predictions are also better calibrated as the red curve is closer to diagonal. Comparisons to SGD on ImageNet are in Table 1. Final numbers for IVON vs AdamW are as follows: 12.6 vs. 13.0 perplexity (lower is better) on GPT-2 (773M), 14.1 vs 14.5 perplexity on GPT-2 (355M), 17.9 vs 18.1 perplexity on GPT-2 (125M), 77.5 vs 75.2 accuracy and 0.022 vs 0.066 ECE (lower is better) on ResNet-50.

2. Challenges of Variational Learning for Large Deep Networks

Variational learning is challenging for large networks due to fundamental differences in its objective to those commonly used in deep learning. Deep learning methods estimate network weights $\boldsymbol{\theta} \in \mathbb{R}^P$ by minimizing empirical risk $\bar{\ell}(\boldsymbol{\theta}) = \sum_{i=1}^N \ell_i(\boldsymbol{\theta})/N$, which is an average over individual losses $\ell_i(\boldsymbol{\theta})$ for N examples. In contrast, variational methods estimate a distribution $q(\boldsymbol{\theta})$ over weights by minimizing

$$\mathcal{L}(q) = \lambda \mathbb{E}_{q(\boldsymbol{\theta})}\left[\bar{\ell}(\boldsymbol{\theta})\right] + \mathbb{D}_{\mathrm{KL}}(q(\boldsymbol{\theta}) \,\|\, p(\boldsymbol{\theta})), \qquad (1)$$

where $p(\boldsymbol{\theta})$ is the prior, $\mathbb{D}_{\mathrm{KL}}(\cdot \,\|\, \cdot)$ the Kullback-Leibler divergence and λ a scaling parameter often set to N, but other values are useful, for example, to handle model misspecification. The objective in Eq. 1 coincides with variational *inference* when $\bar{\ell}(\boldsymbol{\theta})$ is a proper likelihood. We use the term *variational learning* to denote the general case.

Optimization of $\mathcal{L}(q)$ is fundamentally different from that of $\bar{\ell}(\boldsymbol{\theta})$. For instance, the number of parameters of q can be much larger than the size of $\boldsymbol{\theta}$, making the problem harder. The number of parameters of q is doubled for a diagonal-covariance Gaussian $q(\boldsymbol{\theta}) = \mathcal{N}(\boldsymbol{\theta} \,|\, \mathbf{m}, \mathrm{diag}(\boldsymbol{\sigma})^2)$ due to the estimation of two vectors of mean $\mathbf{m} \in \mathbb{R}^P$ and standard deviation $\boldsymbol{\sigma} \in \mathbb{R}^P$, respectively. The optimization is further complicated because of the expectation in Eq. 1, which adds additional noise during the optimization.

Due to these differences, a direct optimization of Eq. 1 remains challenging. The standard approach is to optimize it by using a standard deep learning method, say, SGD,

$$\mathbf{m} \leftarrow \mathbf{m} - \rho \widehat{\nabla}_{\mathbf{m}} \mathcal{L} \qquad \boldsymbol{\sigma} \leftarrow \boldsymbol{\sigma} - \rho \widehat{\nabla}_{\boldsymbol{\sigma}} \mathcal{L},$$

where $\rho > 0$ is the learning rate. This showed promising results in early attempts of variational deep learning with several different stochastic gradient estimators $\widehat{\nabla}$ (Graves, 2011; Blundell et al., 2015). Unfortunately, these methods have been unable to keep up with the growth in scale of deep learning. The lack of progress has been attributed to various causes, such as high-variance in stochastic gradients (Kingma et al., 2015; Wen et al., 2018), issues with the temperature parameter (Wenzel et al., 2020; Noci et al., 2021), and lack of a good prior (Fortuin et al., 2022). Multiple theoretical studies have raised doubts whether variational learning can ever work at all (Trippe & Turner, 2017; Foong et al., 2020; Coker et al., 2022). Altogether, these have led to a belief that there exists an inherent trade-off between accuracy and uncertainty in Bayesian learning.

Progress in variational learning has been made on a different front by using *natural-gradient* methods (Sato, 2001; Hoffman et al., 2013; Khan & Lin, 2017) which have shown promising results on ImageNet (Osawa et al., 2019). Their updates resemble an Adam-like form which makes it easy to tune them at large scale. Yet, the implementation can be tricky and the cost can be much higher than Adam. For example, Osawa et al. (2019) build upon the Variational Online Newton (VON) method of Khan et al. (2018) where they replace the Hessian computation by a Gauss-Newton estimate. They implement the following Adam-like update:

$$\begin{aligned}
\widehat{\mathbf{h}} &\leftarrow \frac{1}{|\mathcal{B}|}\sum_{i\in\mathcal{B}} \nabla \ell_i(\boldsymbol{\theta})^2, \quad \text{where } \boldsymbol{\theta} \sim q, \\
\mathbf{g} &\leftarrow \beta_1 \mathbf{g} + \widehat{\nabla}\bar{\ell}(\boldsymbol{\theta}) + s_0 \mathbf{m}/\lambda, \\
\mathbf{h} &\leftarrow \beta_2 \mathbf{h} + (1-\beta_2)\widehat{\mathbf{h}}, \\
\mathbf{m} &\leftarrow \mathbf{m} - \alpha_t \mathbf{g}/(\mathbf{h}+c), \\
\boldsymbol{\sigma} &\leftarrow 1/\sqrt{\lambda(\mathbf{h}+c)}.
\end{aligned} \qquad (2)$$

Here, a prior $p(\boldsymbol{\theta}) = \mathcal{N}(\boldsymbol{\theta} \,|\, 0, \mathbf{I}/s_0)$ is used. The difficult

computation is in the first line of Eq. 2 where a Gauss-Newton estimate over a minibatch $\mathcal{B}$ is computed at a sample from the Gaussian, while the rest is similar to Adam: the second line is gradient momentum, where $s_0\mathbf{m}/\lambda$ is added due to the prior. The third and fourth line are identical to the scale and parameter vectors updates, respectively. The constant $c = \gamma + s_0/\lambda$ where $\gamma > 0$ is a damping parameter.

The computation of the Gauss-Newton estimate is tricky because it requires per-example squaring, which is not a standard operation in deep learning and could be difficult to implement. In Osawa et al. (2019, Fig. 1), this ends up increasing the cost by a factor of two. The Gauss-Newton estimate also introduces an additional approximation in the variational learning, even though it helps to ensure the positivity of $\mathbf{h}$. Another issue is the use of an additional damping parameter γ which departs from the Bayesian framework.

Ideally, we want a method that directly optimizes Eq. 1 without additional approximations and also seamlessly fits into an Adam-like framework without any significant computational overheads. Methods such as MC-dropout, SWAG, and Laplace do not solve this problem, and rather circumvent it by relying on algorithms that optimize $\bar{\ell}$, not $\mathcal{L}$. The goal of this paper is to propose a method that can match the accuracy of Adam while directly optimizing $\mathcal{L}$.

3. Improved Variational Online Newton

We present the Improved Variational Online Newton (IVON) method by adapting the method of Lin et al. (2020) and introducing practical tricks necessary to achieve good performance at large scale. They propose an improved version of the Bayesian Learning Rule (Khan & Rue, 2021) which ensures positivity of certain variational parameters, such as, the Gaussian variance or scale parameter of a Gamma distribution. For the Gaussian case, they propose an Adam-like update which makes the update in Eq. 2 simpler. Specifically, they use the following Hessian estimate by using the reparameterization trick,

$$\widehat{\mathbf{h}} \leftarrow \widehat{\nabla}\bar{\ell}(\boldsymbol{\theta}) \cdot \frac{\boldsymbol{\theta} - \mathbf{m}}{\boldsymbol{\sigma}^2}, \tag{3}$$

which does not require per-example gradient squares, rather just a single vector multiplication with the minibatch gradient. The above estimate is easy to compute but, unlike the Gauss-Newton estimate, it is not always positive and can make $\mathbf{h}$ in Eq. 2 negative (Khan et al., 2018, App. D). Lin et al. (2020) solve this problem by using Riemannian gradient descent which ensures positivity by adding an extra term in the update of $\mathbf{h}$,

$$\mathbf{h} \leftarrow (1-\rho)\mathbf{h} + \rho\widehat{\mathbf{h}} + \tfrac{1}{2}\rho^2(\mathbf{h} - \widehat{\mathbf{h}})^2/(\mathbf{h} + s_0/\lambda), \tag{4}$$

where $\rho > 0$ is a constant. Positivity holds even when $\widehat{\mathbf{h}}$ are negative, as shown in Lin et al. (2020, Theorem 1).

Algorithm 1 Improved Variational Online Newton (IVON). Hyperparameter setting is described in App. A.

Require: Learning rates $\{\alpha_t\}$, weight-decay $\delta > 0$.
Require: Momentum parameters $\beta_1, \beta_2 \in [0, 1)$.
Require: Hessian init $h_0 > 0$.
Init: $\mathbf{m} \leftarrow$ (NN-weights), $\mathbf{h} \leftarrow h_0$, $\mathbf{g} \leftarrow 0$, $\lambda \leftarrow N$.
Init: $\boldsymbol{\sigma} \leftarrow 1/\sqrt{\lambda(\mathbf{h} + \delta)}$.
Optional: $\alpha_t \leftarrow (h_0 + \delta)\alpha_t$ for all t.

1: **for** $t = 1, 2, \ldots$ **do**
2: $\quad\widehat{\mathbf{g}} \leftarrow \widehat{\nabla}\bar{\ell}(\boldsymbol{\theta})$, where $\boldsymbol{\theta} \sim q$
3: $\quad\widehat{\mathbf{h}} \leftarrow \widehat{\mathbf{g}} \cdot (\boldsymbol{\theta} - \mathbf{m})/\boldsymbol{\sigma}^2$
4: $\quad\mathbf{g} \leftarrow \beta_1\mathbf{g} + (1-\beta_1)\widehat{\mathbf{g}}$
5: $\quad\mathbf{h} \leftarrow \beta_2\mathbf{h} + (1-\beta_2)\widehat{\mathbf{h}} + \frac{1}{2}(1-\beta_2)^2(\mathbf{h} - \widehat{\mathbf{h}})^2/(\mathbf{h} + \delta)$
6: $\quad\bar{\mathbf{g}} \leftarrow \mathbf{g}/(1 - \beta_1^t)$
7: $\quad\mathbf{m} \leftarrow \mathbf{m} - \alpha_t(\bar{\mathbf{g}} + \delta\mathbf{m})/(\mathbf{h} + \delta)$
8: $\quad\boldsymbol{\sigma} \leftarrow 1/\sqrt{\lambda(\mathbf{h} + \delta)}$
9: **end for**
10: **return** $\mathbf{m}, \boldsymbol{\sigma}$

In Alg. 1, we use the two modifications (highlighted in red) to get an improved version of VON, called IVON. The updates closely resemble Adam, but there is a sampling step in line 2 (highlighted in blue) and there is no square-root over $\mathbf{h}$ in line 7. IVON therefore uses a Newton-like update. The Hessian estimator in Eq. 3 is less costly compared to other second-order optimizers (Dauphin et al., 2015; Yao et al., 2021; Liu et al., 2024). It is valid even for losses that are not twice-differentiable (for example, for ReLU activations). These aspects make IVON a unique second-order optimizer with similar costs to Adam.

Below are a few practical tricks needed for good results.

1. Instead of the prior precision s_0, we use the weight-decay regularizer δ as the prior. The scaling parameter λ is set to N, except for finetuning on small datasets.

2. Unlike Lin et al. (2020, Fig. 1), the update of $\mathbf{h}$ does not use δ. We do not debias $\mathbf{h}$ and we update it before $\mathbf{m}$ which has no impact on the performance.

3. The Hessian $\mathbf{h}$ is initialized with a constant h_0. Lin et al. (2020) most likely set it to 0 due to the debiasing step used in their work. We find the initialization to be useful. Too small values can destabilize the training while larger values may give poor performance.

4. When training transformers, it can be helpful to clip the preconditioned gradient in line 7 entrywise to $[-\xi, \xi]$.

5. Optionally, we rescale α_t by $(h_0 + \delta)$ so that the first steps of the algorithm have step-size close to the initial α_t. When clipping is used, this step is omitted.

Dataset / Model	Method	Top-1 Acc. ↑	Top-5 Acc. ↑	NLL ↓	ECE ↓	Brier ↓
ImageNet ResNet-50 (26M params)	AdamW	(2%) $75.16_{\pm 0.14}$	$92.37_{\pm 0.03}$	$1.018_{\pm 0.003}$	$0.066_{\pm 0.002}$	$0.349_{\pm 0.002}$
	SGD	(1%) $76.63_{\pm 0.45}$	$93.21_{\pm 0.25}$	$0.917_{\pm 0.026}$	$0.038_{\pm 0.009}$	$0.326_{\pm 0.006}$
	IVON@mean	$77.30_{\pm 0.08}$	$93.58_{\pm 0.05}$	$0.884_{\pm 0.002}$	$0.035_{\pm 0.002}$	$\mathbf{0.316}_{\pm 0.001}$
	IVON	$\mathbf{77.46}_{\pm 0.07}$	$\mathbf{93.68}_{\pm 0.04}$	$\mathbf{0.869}_{\pm 0.002}$	$\mathbf{0.022}_{\pm 0.002}$	$\mathbf{0.315}_{\pm 0.001}$
TinyImageNet ResNet-18 (11M params)	AdamW	(15%) $47.33_{\pm 0.90}$	$71.54_{\pm 0.95}$	$6.823_{\pm 0.235}$	$0.421_{\pm 0.008}$	$0.913_{\pm 0.018}$
	SGD	(1%) $61.39_{\pm 0.18}$	$82.30_{\pm 0.22}$	$1.811_{\pm 0.010}$	$0.138_{\pm 0.002}$	$0.536_{\pm 0.002}$
	IVON@mean	$\mathbf{62.41}_{\pm 0.15}$	$\mathbf{83.77}_{\pm 0.18}$	$1.776_{\pm 0.018}$	$0.150_{\pm 0.005}$	$0.532_{\pm 0.002}$
	IVON	$\mathbf{62.68}_{\pm 0.16}$	$\mathbf{84.12}_{\pm 0.24}$	$\mathbf{1.528}_{\pm 0.010}$	$\mathbf{0.019}_{\pm 0.004}$	$\mathbf{0.491}_{\pm 0.001}$
TinyImageNet PreResNet-110 (4M params)	AdamW	(11%) $50.65_{\pm 0.0^*}$	$74.94_{\pm 0.0^*}$	$4.487_{\pm 0.0^*}$	$0.357_{\pm 0.0^*}$	$0.812_{\pm 0.0^*}$
	SGD	(2%) $59.39_{\pm 0.50}$	$81.34_{\pm 0.30}$	$2.040_{\pm 0.040}$	$0.176_{\pm 0.006}$	$0.577_{\pm 0.007}$
	IVON@mean	$\mathbf{60.85}_{\pm 0.39}$	$\mathbf{83.89}_{\pm 0.14}$	$1.584_{\pm 0.009}$	$0.053_{\pm 0.002}$	$\mathbf{0.514}_{\pm 0.003}$
	IVON	$\mathbf{61.25}_{\pm 0.48}$	$\mathbf{84.13}_{\pm 0.17}$	$\mathbf{1.550}_{\pm 0.009}$	$\mathbf{0.049}_{\pm 0.002}$	$\mathbf{0.511}_{\pm 0.003}$
CIFAR-100 ResNet-18 (11M params)	AdamW	(11%) $64.12_{\pm 0.43}$	$86.85_{\pm 0.51}$	$3.357_{\pm 0.071}$	$0.278_{\pm 0.005}$	$0.615_{\pm 0.008}$
	SGD	(1%) $74.46_{\pm 0.17}$	$92.66_{\pm 0.06}$	$1.083_{\pm 0.007}$	$0.113_{\pm 0.001}$	$0.376_{\pm 0.001}$
	IVON@mean	$74.51_{\pm 0.24}$	$92.74_{\pm 0.19}$	$1.284_{\pm 0.013}$	$0.152_{\pm 0.003}$	$0.399_{\pm 0.002}$
	IVON	$\mathbf{75.14}_{\pm 0.34}$	$\mathbf{93.30}_{\pm 0.19}$	$\mathbf{0.912}_{\pm 0.009}$	$\mathbf{0.021}_{\pm 0.003}$	$\mathbf{0.344}_{\pm 0.003}$
CIFAR-100 PreResNet-110 (4M params)	AdamW	(10%) $65.88_{\pm 0.84}$	$88.34_{\pm 0.56}$	$2.893_{\pm 0.088}$	$0.258_{\pm 0.006}$	$0.578_{\pm 0.014}$
	SGD	(2%) $74.19_{\pm 0.11}$	$92.41_{\pm 0.14}$	$1.204_{\pm 0.012}$	$0.137_{\pm 0.002}$	$0.393_{\pm 0.004}$
	IVON@mean	$75.23_{\pm 0.23}$	$93.45_{\pm 0.16}$	$1.149_{\pm 0.010}$	$0.136_{\pm 0.002}$	$0.380_{\pm 0.003}$
	IVON	$\mathbf{75.81}_{\pm 0.18}$	$\mathbf{93.93}_{\pm 0.19}$	$\mathbf{0.884}_{\pm 0.007}$	$\mathbf{0.030}_{\pm 0.003}$	$\mathbf{0.336}_{\pm 0.001}$

Table 1: IVON improves both accuracy and uncertainty over SGD and AdamW. Improvements in accuracy by IVON are shown in red. The performance of AdamW is not good on the smaller datasets likely due to overfitting when training for 200 epochs. IVON does not have this issue. Additional results are in the appendix in Tables 9 to 11 and Table 13.

Momentum β_1, learning rate α_t and weight-decay δ can be set in the same fashion as for standard optimizers, as well as minibatch size and clipping radius ξ. β_2 typically needs to be closer to one as in Adam, for instance, values of $\beta_2 = 0.99995$ work well. h_0 is typically around 0.01 to 1, and setting λ is also easy, as discussed above. This makes obtaining good results with IVON often very easy. A detailed guide for hyperparameter setting is in App. A.

IVON can be easily modified to accommodate multi-GPU training. Each GPU device can use different Monte-Carlo (MC) samples, which reduces the variance (Kingma et al., 2015). Moreover, multiple MC samples per device can also be used. These modifications can be realized by simply replacing the calculations of $\widehat{\mathbf{g}}$ and $\widehat{\mathbf{h}}$ in line 2 and 3 of Alg. 1 by the following averages over J devices and a total of S MC samples drawn on each device:

$$\widehat{\mathbf{g}} = \frac{\sum_{j,s} \widehat{\nabla}\bar{\ell}(\boldsymbol{\theta}_j^{(s)})}{J \cdot S}, \quad \widehat{\mathbf{h}} = \frac{\sum_{j,s} \widehat{\nabla}\bar{\ell}(\boldsymbol{\theta}_j^{(s)})(\boldsymbol{\theta}_j^{(s)} - \mathbf{m})}{J \cdot S \cdot \boldsymbol{\sigma}^2}.$$

Here, we use a different $\boldsymbol{\theta}_j^{(s)} \sim q$ on each device j and for each MC sample s. Both sums can be implemented as running averages for better memory-efficiency.

We implement IVON as a drop-in replacement for Adam in PyTorch, where only two lines need to be added (marked red below) to draw multiple MC samples:

```
for inputs, targets in dataloader:
 for _ in range(num_mc_samples):
  with optimizer.sampled_params(train=True):
   optimizer.zero_grad()
   outputs = model(inputs)
   loss = loss_fn(outputs, targets)
   loss.backward()
 optimizer.step()
```

The first red line is often not needed because a single sample can already give reasonable results.

4. IVON is Effective for Large Deep Networks

We show that IVON effectively trains large deep networks from scratch (Sec. 4.1) and enables many downstream applications, such as predictive uncertainty (Sec. 4.2), fine-tuning and model merging (Sec. 4.3), as well as predicting generalization and finding influential training examples (Sec. 4.4). We perform ablation studies on computational efficiency (App. B.1), the choice of Hessian estimator (App. B.2) and initialization (App. B.3). In the following, we refer by IVON@mean to the prediction using $\mathbf{m}$ as the weights, whereas IVON denotes a model average with 64 samples drawn from the posterior learned by IVON.

4.1. Better Scalability and Generalization

Here, we show how IVON scalably trains large models from scratch. First, we train LLMs with up to 773M parameters from scratch on ca. 50B tokens. Then, we show

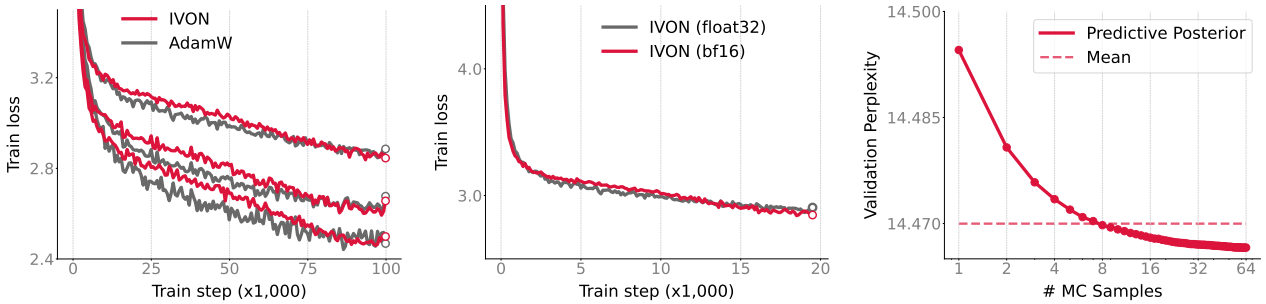

(a) Training loss on OpenWebText (b) Low precision training (c) Predictive posterior

Figure 2: Panel (a) shows that, when training GPT-2, IVON not only improves upon AdamW in terms of validation perplexity but also converges to matching or even better training loss than AdamW. Panel b shows that IVON provides stable training when using low-precision (bf16) floating point numbers. Panel (c) shows that averaging predictions over IVON's posterior further improves the validation perplexity on GPT-2, when a sufficient number of samples is used (> 8).

improved accuracy and uncertainty for various image classification models, for example, ResNets with 26M parameters at ImageNet-scale. Additional results on smaller recurrent neural networks with 2M parameters are in App. D.1.

4.1.1. Pretraining language models

Pretraining transformer language models (Vaswani et al., 2017) with variational learning has been challenging and no large-scale result exists so far. We show that IVON can train large language models at scale. We train models following the GPT-2 architecture (Radford et al., 2019) for 49.2 billion tokens in total on the OpenWebText corpus (Gokaslan & Cohen, 2019). We use the same hyperparameters for AdamW as prior work (Liu et al., 2024). For IVON, we set them by grid search on a smaller model. We pretrain from scratch three models with parameter sizes of 125M, 355M ("GPT-2-medium"), and 773M ("GPT-2-large"), respectively. We use gradient clipping to stabilize the training. Details are in App. C.1.

As shown in Fig. 1(a), for the three models, the validation perplexities are reduced from 18.1 to 17.9, from 14.5 to 14.1 and from 13.0 to 12.6, respectively. Fig. 2(a) further shows the same trend for training loss. Fig. 2(b) shows stable training with bf16 precision, and Fig. 2(c) shows that sampling multiple models from IVON's posterior further improves performance when a sufficient number of samples is used. Overall, we see effectiveness for training large Transformers from scratch on large datasets.

4.1.2. Image classification

We compare IVON to AdamW and SGD (with momentum) for image classification on various models and benchmarks. Table 1 shows that IVON improves upon both AdamW and the stronger SGD baseline in terms of both accuracy and uncertainty, here measured by negative log-likelihood (NLL), expected calibration error (ECE), and Brier score. We also find that IVON does not overfit on smaller tasks, unlike AdamW which tends to overfit on TinyImageNet and CIFAR-100. This holds on various datasets and models trained for 200 epochs. We show two of them here. First, we show ResNet-50 with around 25.6M parameters (He et al., 2016a) on ImageNet-1k which has around 1.2M images with 1000 classes. Second, we show ResNet-18 with 11M parameters and PreResNet-110 with 4M parameters on both TinyImageNet and CIFAR-100. We list further details on the experiments in App. C.2 along with more results using DenseNet-121 and ResNet-20 on other datasets, such as CIFAR-10. There too, we find improvements in both accuracy and uncertainty.

We hypothesize that these improvements are partly due to flat-minima seeking properties of variational learning. Methods aimed to find flat minima, such as sharpness-aware minimization (SAM) (Foret et al., 2021), have recently gained in popularity to boost test-accuracy. Möllenhoff & Khan (2023) have shown that SAM optimizes a relaxation of the expected loss in Eq. 1. Our results here indicate that similar improvements can be obtained by directly optimizing the variational objective and without using any relaxations.

4.2. Posterior Averaging for Predictive Uncertainty

Variational learning naturally allows for improved predictive uncertainties, because we can average predictions of several $\boldsymbol{\theta}$ sampled from the posterior. Unlike other Bayesian Deep Learning (BDL) methods, no postprocessing or model architecture changes are required for this. In the following, we compare IVON to AdamW, SGD, Bayes-by-Backprop (BBB), linearized last-layer Laplace (referred to as Laplace), MC Dropout (referred to as MC-D), SWAG, VOGN and deep ensembles (Lakshminarayanan et al., 2017). We con-

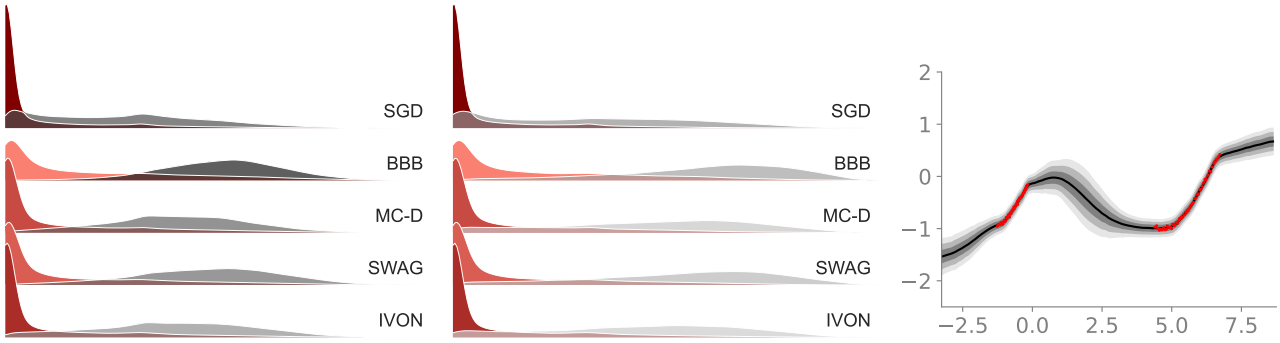

(a) CIFAR-10 on SVHN (b) CIFAR-10 on Flowers102 (c) IVON in-between uncertainty

Figure 3: In panel (a) and (b), we see that IVON's histogram of predictive entropy has a high peak similar to SGD for in-domain data (red, CIFAR-10) but at the same time is spread out widely similar to the other Bayesian deep learning methods for out-of-domain data (gray). The colors are shaded proportional to the height of the peak, that is, darker red and gray indicates a higher peak. In panel (c), we see that IVON can handle in-between uncertainty well, which has been shown to be challenging for variational methods by Foong et al. (2019).

	Acc. (%) ↑	NLL ↓	ECE ↓	Brier ↓
AdamW	$90.04_{\pm 0.27}$	$0.589_{\pm 0.018}$	$0.074_{\pm 0.002}$	$0.170_{\pm 0.004}$
SGD	$91.86_{\pm 0.14}$	$0.288_{\pm 0.015}$	$0.040_{\pm 0.004}$	$0.126_{\pm 0.004}$
BBB	$91.09_{\pm 0.16}$	$0.289_{\pm 0.005}$	$0.053_{\pm 0.001}$	$0.139_{\pm 0.002}$
Laplace	$91.52_{\pm 0.37}$	$0.284_{\pm 0.008}$	$0.033_{\pm 0.002}$	$0.129_{\pm 0.004}$
MC-D	$91.85_{\pm 0.17}$	$0.242_{\pm 0.004}$	$\mathbf{0.008}_{\pm 0.002}$	$0.120_{\pm 0.002}$
SWAG	$92.45_{\pm 0.23}$	$0.230_{\pm 0.002}$	$0.024_{\pm 0.002}$	$0.112_{\pm 0.002}$
VOGN	$92.37_{\pm 0.23}$	$0.226_{\pm 0.005}$	$\mathbf{0.008}_{\pm 0.001}$	$0.111_{\pm 0.003}$
IVON	$\mathbf{92.71}_{\pm 0.07}$	$\mathbf{0.219}_{\pm 0.002}$	$\mathbf{0.008}_{\pm 0.001}$	$\mathbf{0.108}_{\pm 0.001}$
Deep Ens.	$93.57_{\pm 0.16}$	$0.198_{\pm 0.003}$	$\mathbf{0.014}_{\pm 0.001}$	$0.096_{\pm 0.001}$
Multi-IVON	$\mathbf{94.37}_{\pm 0.13}$	$\mathbf{0.179}_{\pm 0.002}$	$0.029_{\pm 0.001}$	$\mathbf{0.087}_{\pm 0.001}$

Table 2: IVON's predictive uncertainty is better than other baselines for in-domain examples. Multi-IVON is a mixture-of-Gaussian ensemble which further improves the performance and is competitive with a deep ensemble.

	FPR@95% ↓	Det. Err. ↓	AUROC ↑	AUPR-In ↑	AUPR-Out ↑
SVHN, see Fig. 3(a)					
SGD	$20.7_{\pm 1.6}$	$18.8_{\pm 0.9}$	$86.7_{\pm 1.0}$	$81.8_{\pm 1.4}$	$91.8_{\pm 0.7}$
BBB	$24.5_{\pm 0.7}$	$17.8_{\pm 0.3}$	$87.0_{\pm 0.3}$	$83.4_{\pm 0.4}$	$91.3_{\pm 0.4}$
Laplace	$19.8_{\pm 1.7}$	$18.8_{\pm 1.0}$	$86.9_{\pm 1.1}$	$81.9_{\pm 1.5}$	$92.0_{\pm 0.8}$
MC-D	$20.7_{\pm 1.3}$	$\mathbf{17.0}_{\pm 0.6}$	$88.0_{\pm 0.8}$	$84.6_{\pm 0.9}$	$92.1_{\pm 0.7}$
SWAG	$19.8_{\pm 2.2}$	$\mathbf{16.6}_{\pm 1.0}$	$\mathbf{88.9}_{\pm 1.1}$	$\mathbf{85.3}_{\pm 1.2}$	$93.0_{\pm 0.9}$
VOGN	$\mathbf{17.2}_{\pm 1.0}$	$\mathbf{16.5}_{\pm 0.4}$	$\mathbf{89.3}_{\pm 0.6}$	$\mathbf{85.3}_{\pm 0.6}$	$\mathbf{93.5}_{\pm 0.5}$
IVON	$\mathbf{17.4}_{\pm 0.8}$	$\mathbf{16.6}_{\pm 0.5}$	$\mathbf{89.2}_{\pm 0.4}$	$\mathbf{85.2}_{\pm 0.6}$	$\mathbf{93.4}_{\pm 0.4}$
Flowers102, see Fig. 3(b)					
SGD	$22.1_{\pm 0.5}$	$20.7_{\pm 0.4}$	$86.3_{\pm 0.3}$	$92.1_{\pm 0.2}$	$75.4_{\pm 0.4}$
BBB	$22.2_{\pm 0.8}$	$19.5_{\pm 0.7}$	$88.2_{\pm 0.7}$	$93.1_{\pm 0.5}$	$79.8_{\pm 0.9}$
Laplace	$20.5_{\pm 1.1}$	$20.1_{\pm 0.6}$	$86.9_{\pm 0.7}$	$92.4_{\pm 0.4}$	$76.4_{\pm 1.3}$
MC-D	$20.3_{\pm 0.8}$	$19.6_{\pm 1.1}$	$87.8_{\pm 0.9}$	$93.0_{\pm 0.7}$	$78.4_{\pm 1.1}$
SWAG	$19.5_{\pm 0.8}$	$\mathbf{18.1}_{\pm 0.5}$	$\mathbf{89.3}_{\pm 0.6}$	$\mathbf{93.9}_{\pm 0.4}$	$\mathbf{81.0}_{\pm 0.9}$
VOGN	$\mathbf{18.1}_{\pm 0.8}$	$\mathbf{18.3}_{\pm 0.3}$	$\mathbf{89.0}_{\pm 0.4}$	$\mathbf{93.8}_{\pm 0.3}$	$\mathbf{80.3}_{\pm 0.7}$
IVON	$\mathbf{17.8}_{\pm 0.5}$	$\mathbf{18.1}_{\pm 0.5}$	$\mathbf{89.0}_{\pm 0.5}$	$\mathbf{93.8}_{\pm 0.3}$	$\mathbf{80.2}_{\pm 0.8}$

Table 3: IVON gives good results for OOD detection using a ResNet-20 mode trained on CIFAR-10. The model is evaluated on SVHN and Flowers102.

sider both in-domain and out-of-domain (OOD) settings. We report common metrics from existing benchmarks (Liang et al., 2018; Snoek et al., 2019). Further details on the experimental setup are in App. C.3.

4.2.1. In-domain comparisons

To evaluate in-domain uncertainty, we train and evaluate ResNet-20 models (He et al., 2016a) on the smaller CIFAR-10 dataset. We choose smaller datasets because it is difficult to apply BBB on larger problems. Results are reported in Table 2. Overall, all BDL baselines, except for BBB which is known to underperform, have significantly better performance than SGD and AdamW. Among all non-ensemble approaches, IVON stands out in both accuracy and uncertainty metrics.

Deep ensembles made up of five models from different SGD runs clearly improve over the non-ensemble methods. We compare them to a similar version of IVON with a mixture-of-Gaussian posterior, constructed from five independently-trained IVON models. This is referred to as Multi-IVON in Table 2, where we find it to outperform deep ensembles. These results altogether confirm the quality of uncertainty estimates obtained with IVON.

4.2.2. Out-of-domain (OOD) comparisons

Next, we consider the OOD case by reusing the CIFAR-10 models on data from a different domain. While we would expect the model to be certain for correct in-domain predictions, it should be less so for out-of-domain examples. This would allow for distinguishing the CIFAR-10 data

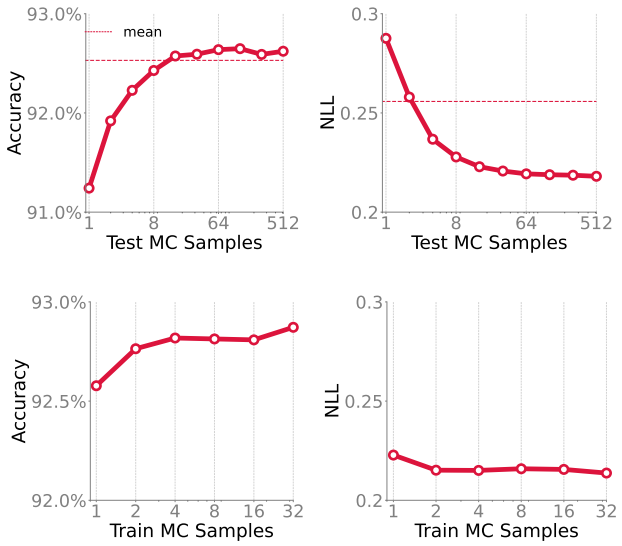

Figure 4: Using more MC samples during inference (top row) or training (bottom row) can improve both accuracy and NLL, here plotted for ResNet-20 on CIFAR-10.

from OOD samples, for which we use the street view house number (SVHN) (Netzer et al., 2011) and the 102 Flowers dataset (Nilsback & Zisserman, 2008, Flowers102).

Table 3 shows that IVON is consistently better at distinguishing OOD examples from SVHN and Flowers102 from in-domain CIFAR-10 data. These results are further illustrated by the predictive entropy plots in Figs. 3(a) and 3(b). In these plots, for in-domain data (shown in red), IVON's histogram has a similarly high peak as SGD, but for out-of-domain data (shown in gray) it is much more spread out than SGD. While the other Bayesian deep learning method's histograms are also spread out for OOD data, they struggle to achieve a high peak for in-domain data. Overall, IVON's histogram has the most clear separation between in-domain data and out-of-domain data. As illustrated in Fig. 3(c), IVON's predictive posterior also gives good in-between uncertainty which has been challenging for other variational methods (Foong et al., 2019). We show further distribution shift experiments in App. D.2.

4.2.3. MC SAMPLES FOR AVERAGING

We find consistent improvements when using more MC samples both during training and inference, but eventually improvements saturate and deliver diminishing returns. Fig. 4 (top row) shows that, for ResNet-20 on CIFAR-10, multiple test samples for prediction improves over the prediction using only the mean, especially in terms of NLL. Similarly, using multiple samples during training improves both accuracy and uncertainty (bottom row in Fig. 4).

	MNLI	QNLI	QQP	RTE	SST2	MRPC	CoLA	STS-B
DeBERTAv3 (440M params)								
AdamW	91.3	**95.7**	**93.1**	91.0	96.5	91.0	74.8	92.4
IVON@mean	**91.6**	**95.7**	93.0	**91.7**	**96.9**	**91.9**	**75.1**	**92.6**
AdamW†	91.8	96.0	93.0	92.7	96.9	92.2	75.3	93.0
RoBERTa (125M params)								
AdamW	87.7	**92.8**	**90.9**	**80.9**	94.8	85.8	**63.6**	90.6
IVON@mean	**87.8**	92.6	90.8	80.6	**95.0**	**87.3**	63.3	**90.8**

Table 4: (Top) IVON generally gives better results compared to AdamW for finetuning on $\text{DeBERTAv3}_{\text{large}}$. Better numbers are reported by He et al. (2023) (indicated by AdamW†) but we are not able to reproduce them. (Bottom) Similar results for $\text{RoBERTa}_{\text{base}}$ where performances are comparable but IVON is marginally better on average.

4.2.4. NEURIPS 2021 COMPETITION

An earlier version of IVON won first place in both tracks of the NeurIPS 2021 competition on approximate inference in Bayesian deep learning (Wilson et al., 2022). The methods were evaluated by their difference in predictions to those of a 'ground-truth' posterior computed on hundreds of TPUs. The winning solution used Multi-IVON (same as Table 2). We summarize the results of the challenge and the differences of the earlier version to Alg. 1 in App. D.3.

4.3. Finetuning and Model Merging

We now demonstrate the usefulness of IVON for finetuning and model-merging. Intuitively, the learned variance $\boldsymbol{\sigma}^2$ (used to adapt the learning rate) should improve finetuning by favoring directions that are flatter. It should also be useful to improve Fisher/Hessian-based model merging, for instance, those discussed by Daheim et al. (2024).

4.3.1. FINETUNING PRETRAINED LANGUAGE MODELS

We compare performance on finetuning of a large masked-language model DeBERTAv3 (He et al., 2023) using AdamW and IVON on GLUE (Wang et al., 2018). Similarly to previous work (Devlin et al., 2019), we do not include the WNLI dataset. DeBERTAv3 has 440M parameters and we finetune the full model using a publicly available checkpoint that was initially trained with AdamW. The results are shown in the top rows of Table 4 where we see that IVON generally improves upon AdamW; all tasks are for classification except STS-B which is a regression tasks. For comparison, we also include results from He et al. (2023) (indicated by AdamW†) which show higher scores but we are unable to reproduce them. Bottom row shows similar results for RoBERTa (Liu et al., 2019), where IVON performs more comparably to AdamW but still gives marginally better results on average. Experimental details are in App. C.4.

	IMDB	Yelp	RT	SST2	Amazon	Avg.	Overhead
SG	93.5	97.0	89.7	92.8	96.6	93.9	100%
IVON	93.6	96.9	89.8	92.8	96.7	94.0	0%

Table 5: IVON reduces the cost of Hessian-based model-merging while giving comparable results to an existing method which requires an extra post-training run through the full data to compute the square-gradients (SG). For IVON, we simply use $\mathbf{h}$ obtained during training which has zero overhead (indicated in last column with 0%).

4.3.2. Merging masked-language models

We repeat the experiments by Daheim et al. (2024) to merge finetuned RoBERTa models on IMDB, Amazon, Yelp, RottenTomatoes, and SST2. Given pretrained weights $\boldsymbol{\theta}_0$, they use the following method to merge T finetuned models $\boldsymbol{\theta}_t$,

$$\boldsymbol{\theta}_{\text{merged}} = \boldsymbol{\theta}_0 + \sum_{t=1}^{T} \frac{\mathbf{h}_0 + \mathbf{h}_t}{\mathbf{h}_0 + \sum_{t'=1}^{T} \mathbf{h}_{t'}} (\boldsymbol{\theta}_t - \boldsymbol{\theta}_0),$$

where $\mathbf{h}_t$ is the diagonal of the Hessian at the t'th model. For IVON, we use the vector $\mathbf{h}$ as the Hessian estimate. We compare it to the squared gradient (SG) estimator: $\mathbf{h}_t = \sum_i [\nabla \hat{\ell}_i(\boldsymbol{\theta}_t)]^2$. The loss $\hat{\ell}_i$ here is the same as ℓ_i but uses labels sampled from the model. The estimator is related to Laplace's method (Daheim et al., 2024) and requires an extra post-training run over the full dataset. For both methods, we set $\mathbf{h}_0$ using the SG method because IVON is not used during pretraining. We use same settings as App. C.4.

Table 5 shows that both estimates perform similarly, despite IVON not needing an extra pass through the dataset (indicated by 0% overhead in the last column). We expect the results to get even better when the model is pretrained with IVON, because then $\mathbf{h}_0$ is also estimated during pretraining.

4.4. Estimating Generalization and Sensitivity to Data

We demonstrate the usefulness of IVON to faithfully predict generalization performance and also understand sensitivity to training data. The former is useful for training diagnostics and early stopping, while the latter is useful for model understanding and data cleaning. To do so, we simply plug-in the variance estimate $\boldsymbol{\sigma}^2$ obtained during IVON's training into the influence measures derived by Nickl et al. (2023). We find this simple method to give good results compared to existing influence function methods (Koh & Liang, 2017) that are known to be fragile for large deep networks (Basu et al., 2021) but also are not designed to work during training.

4.4.1. Predicting generalization Performance

We use IVON to estimate the Leave-One-Out (LOO) Cross-Validation loss as a measure of generalization performance. Given a $\boldsymbol{\theta}$ during training, Nickl et al. (2023) use its prediction error e_i and prediction variance v_i on the i'th example

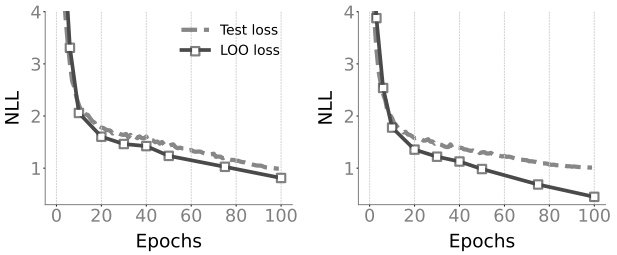

(a) IVON (b) AdamW

Figure 5: Panel (a) shows that, for ImageNet, IVON's LOO estimate (solid line with square markers) accurately follows the loss trajectory on an unseen test set (dashed line). Panel (b) shows that same for AdamW which is not as good.

to estimate the deviation $\boldsymbol{\theta}^{\setminus i}$ obtained by removing the same i'th example. This is then used to estimate the LOO loss,

$$\text{LOO}(\boldsymbol{\theta}) = \sum_{i=1}^{N} \ell(f_i^{\setminus i}) \approx \sum_{i=1}^{N} \ell(f_i + v_i e_i),$$

where f_i and $f_i^{\setminus i}$ are predictions by using $\boldsymbol{\theta}$ and $\boldsymbol{\theta}^{\setminus i}$, respectively, for the i'th example and we denote $\ell(f_i) = \ell_i(\boldsymbol{\theta})$. IVON's variance $\boldsymbol{\sigma}^2$ is expected to improve the predictive variance v_i (see App. C.5) and this experiment demonstrates the effectiveness of the variance estimate compared to the Squared-Gradient (SG) estimate used in Adam.

Fig. 5 shows the results on ImageNet (setup similar to the one shown in Table 1). We see that IVON's LOO estimate closely follows the (true) loss on an unseen test set. The LOO objective is evaluated using sensitivities calculated from IVON during training. Similar estimates obtained with AdamW do not work as well, for instance, they converge close to 0 which reflects the training loss more than the test loss. Details of the method used for AdamW are given in App. C.5. Each plot shows LOO at regular intervals indicated with the markers. Additional results for many other architectures on CIFAR-10 are given in App. D.4.

4.4.2. Sensitivity to Training Data

We present qualitative results to estimate sensitivity of the model to its training data. Similarly to Nickl et al. (2023), we define the sensitivity measure to be the absolute value of $v_i e_i$. Higher values suggest higher sensitivities. Because the sensitivity estimates are obtained by multiplying e_i and v_i, we expect low sensitivity images to be those predicted correctly with high confidence, that is, they should be *typical* images. In contrast, high sensitivity images are the ones with high prediction error and/or high variance, which in general would be *atypical* ones (mislabeled or ambiguous).

Fig. 6 illustrates low- and high-sensitivity images for the "great white shark" class on ImageNet (details in App. C.5).

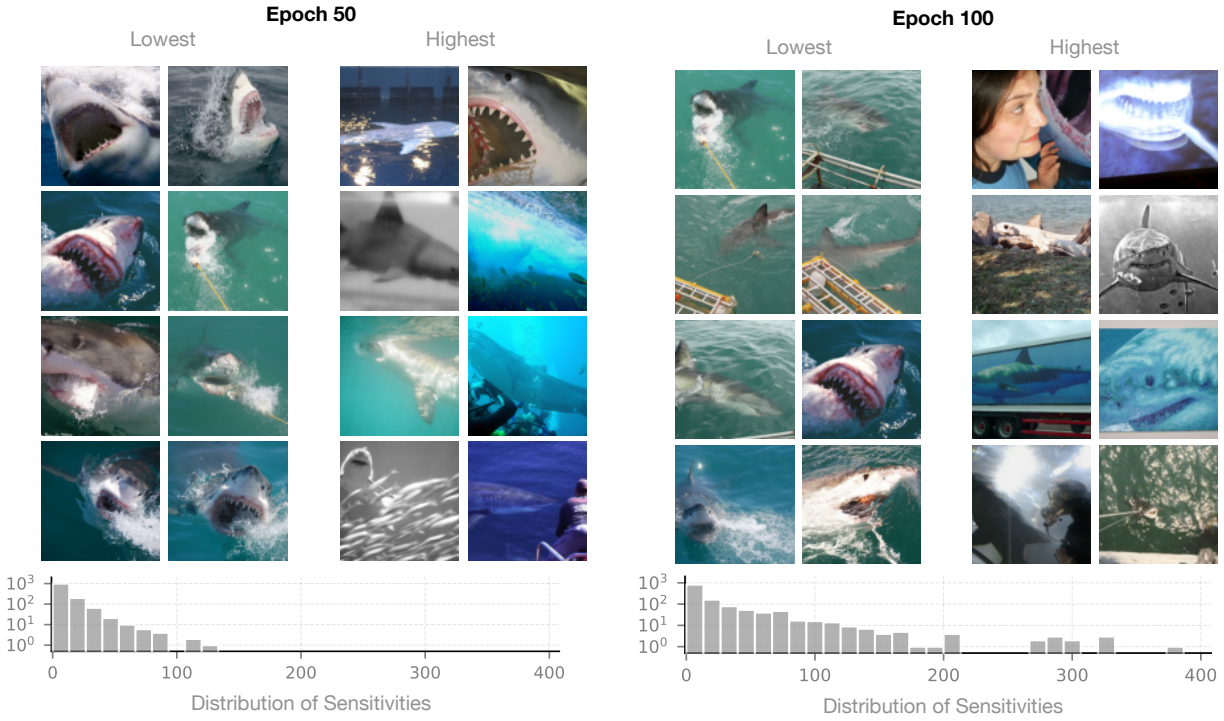

Figure 6: We use IVON to estimate sensitivity of ResNet-50 to examples in the ImageNet dataset, and visualize high and low sensitivity images for the "great white shark" class at two epochs of 50 and 100 respectively. Low-sensitivity examples are mostly typical shark images, while high-sensitivity ones are unusual images, possibly containing mislabeled or ambiguous examples. For instance, one picture shows more prominently the face of a woman than the shark. The high-sensitivity examples also continue to evolve when going from 50 to 100 epochs (the distribution of sensitivities flattens), perhaps indicating that the model tends to learn them a bit later in the training.

We show two epochs (50 and 100, respectively). Already at 50 epochs, low-sensitivity examples show the regular shark pattern, but high-sensitivity examples keep appearing as the training progresses (the distribution of sensitivities flattens). At epoch 100, we see some clear examples containing atypical images, for instance, a picture of a woman's face featured more prominently than the shark.

5. Discussion and Limitations

We show the effectiveness of variational learning for training large networks. Especially our results on GPT-2 and other LLMs are first of their kind and clearly demonstrate the potential that variational learning holds. We also discussed many new use cases where we consistently find benefits by switching to a variational approach. We expect our results to be useful for future work on showing the effectiveness of Bayesian learning in general.

Although we borrow practical tricks from deep learning, not all of them are equally useful for IVON, for example, we find that IVON does not go well with batch normalization layers (Ioffe & Szegedy, 2015). Future research should explore this limitation and investigate the reasons behind the effectiveness of some practical tricks. Using MC samples in variational learning increases the computation cost and we believe it is difficult to fix this problem. For this, deterministic versions of the variational objective can be useful, for example, those discussed by Möllenhoff & Khan (2023) but this is a potential direction for future research.

IVON can be easily modified to learn flexible posterior forms (Lin et al., 2019). Our Multi-IVON method in this paper uses a simple mixture distribution, but we expect further improvements by using other types of mixtures and also by learning the mixing distribution. We expect this aspect of IVON to help researchers further investigate the benefits of Bayesian principles to improve deep learning.

Acknowledgements

This work is supported by JST CREST Grant Number JPMJCR2112. This research work has been funded by the German Federal Ministry of Education and Research and the Hessian Ministry of Higher Education, Research, Science and the Arts within their joint support of the National Re-

search Center for Applied Cybersecurity ATHENE. Y. Shen and D. Cremers are supported by the Munich Center for Machine Learning (MCML) and the ERC Advanced Grant SIMULACRON. Some of the experiments were carried out with the TSUBAME3.0 supercomputer at the Tokyo Institute of Technology.

We thank Happy Buzaaba for first experiments on finetuning transformers with IVON and Keigo Nishida, Falko Helm and Hovhannes Tamoyan for feedback on a draft of this paper. Finally, we thank the organizers of the NeurIPS 2021 Competition on Approximate Inference in Bayesian Deep Learning.

Impact Statement

This paper presents work whose goal is to advance the field of Machine Learning. There are many potential societal consequences of our work, none which we feel must be specifically highlighted here.

References

Basu, S., Pope, P., and Feizi, S. Influence functions in deep learning are fragile. In *International Conference on Learning Representations (ICLR)*, 2021.

Blundell, C., Cornebise, J., Kavukcuoglu, K., and Wierstra, D. Weight uncertainty in neural networks. In *International Conference on Machine Learning (ICML)*, 2015.

Cer, D., Diab, M., Agirre, E., Lopez-Gazpio, I., and Specia, L. SemEval-2017 task 1: Semantic textual similarity multilingual and crosslingual focused evaluation. In *International Workshop on Semantic Evaluation (SemEval-2017)*, 2017.

Cho, K., Van Merriënboer, B., Gulcehre, C., Bahdanau, D., Bougares, F., Schwenk, H., and Bengio, Y. Learning phrase representations using RNN encoder-decoder for statistical machine translation. In *Conference on Empirical Methods in Natural Language Processing*, 2014.

Coker, B., Bruinsma, W. P., Burt, D. R., Pan, W., and Doshi-Velez, F. Wide mean-field Bayesian neural networks ignore the data. In *International Conference on Artificial Intelligence and Statistics (AISTATS)*, 2022.

Daheim, N., Möllenhoff, T., Ponti, E. M., Gurevych, I., and Khan, M. E. Model merging by uncertainty-based gradient matching. In *International Conference on Learning Representations (ICLR)*, 2024.

Dauphin, Y., De Vries, H., and Bengio, Y. Equilibrated adaptive learning rates for non-convex optimization. *Advances in Neural Information Processing Systems (NeurIPS)*, 2015.

Daxberger, E., Kristiadi, A., Immer, A., Eschenhagen, R., Bauer, M., and Hennig, P. Laplace redux – effortless Bayesian deep learning. In *Advances in Neural Information Processing Systems (NeurIPS)*, 2021.

Delaunoy, A. and Louppe, G. SAE: Sequential anchored ensembles. *arXiv:2201.00649*, 2021.

Deng, J., Dong, W., Socher, R., Li, L.-J., Li, K., and Fei-Fei, L. ImageNet: A large-scale hierarchical image database. In *IEEE Conference on Computer Vision and Pattern Recognition (CVPR)*, 2009.

Devlin, J., Chang, M.-W., Lee, K., and Toutanova, K. BERT: Pre-training of deep bidirectional transformers for language understanding. In *Conference of the North American Chapter of the Association for Computational Linguistics: Human Language Technologies, Volume 1 (Long and Short Papers)*, 2019.

Dolan, W. B. and Brockett, C. Automatically constructing a corpus of sentential paraphrases. In *International Workshop on Paraphrasing (IWP2005)*, 2005.

Foong, A., Burt, D., Li, Y., and Turner, R. On the expressiveness of approximate inference in Bayesian neural networks. *Advances in Neural Information Processing Systems*, 33, 2020.

Foong, A. Y., Li, Y., Hernández-Lobato, J. M., and Turner, R. E. 'In-Between' uncertainty in Bayesian neural networks. *ICML Workshop on Uncertainty and Robustness in Deep Learning*, 2019.

Foret, P., Kleiner, A., Mobahi, H., and Neyshabur, B. Sharpness-aware minimization for efficiently improving generalization. In *International Conference on Learning Representations (ICLR)*, 2021.

Fortuin, V., Garriga-Alonso, A., Wenzel, F., Rätsch, G., Turner, R., van der Wilk, M., and Aitchison, L. Bayesian neural network priors revisited. In *International Conference on Learning Representations (ICLR)*, 2022.

Gal, Y. and Ghahramani, Z. Dropout as a Bayesian approximation: Representing model uncertainty in deep learning. In *International Conference on Machine Learning (ICML)*, 2016.

Gokaslan, A. and Cohen, V. OpenWebText corpus, 2019. URL `http://Skylion007.github.io/OpenWebTextCorpus`.

Graves, A. Practical variational inference for neural networks. In *Advances in Neural Information Processing Systems (NeurIPS)*, 2011.

He, K., Zhang, X., Ren, S., and Sun, J. Deep residual learning for image recognition. In *IEEE Conference on Computer Vision and Pattern Recognition (CVPR)*, 2016a.

He, K., Zhang, X., Ren, S., and Sun, J. Identity mappings in deep residual networks. In *European Conference on Computer Vision (ECCV)*, 2016b.

He, P., Gao, J., and Chen, W. DeBERTav3: Improving deBERTa using ELECTRA-style pre-training with gradient-disentangled embedding sharing. In *International Conference on Learning Representations (ICLR)*, 2023.

Hendrycks, D. and Dietterich, T. G. Benchmarking neural network robustness to common corruptions and perturbations. In *International Conference on Learning Representations (ICLR)*, 2019.

Hendrycks, D. and Gimpel, K. Gaussian error linear units (GELUs). *arXiv preprint arXiv:1606.08415*, 2016.

Hernández-Lobato, J. M. and Adams, R. Probabilistic backpropagation for scalable learning of Bayesian neural networks. In *International Conference on Machine Learning (ICML)*, 2015.

Hoffman, M. D., Blei, D. M., Wang, C., and Paisley, J. Stochastic variational inference. *J. Mach. Learn. Res. (JMLR)*, 14(5), 2013.

Hoffmann, J., Borgeaud, S., Mensch, A., Buchatskaya, E., Cai, T., Rutherford, E., de las Casas, D., Hendricks, L. A., Welbl, J., Clark, A., Hennigan, T., Noland, E., Millican, K., van den Driessche, G., Damoc, B., Guy, A., Osindero, S., Simonyan, K., Elsen, E., Vinyals, O., Rae, J. W., and Sifre, L. An empirical analysis of compute-optimal large language model training. In *Advances in Neural Information Processing Systems (NeurIPS)*, 2022.

Huang, G., Liu, Z., van der Maaten, L., and Weinberger, K. Q. Densely connected convolutional networks. In *IEEE Conference on Computer Vision and Pattern Recognition (CVPR)*, 2017.

Ioffe, S. and Szegedy, C. Batch normalization: Accelerating deep network training by reducing internal covariate shift. In *International Conference on Machine Learning*, 2015.

Izmailov, P., Vikram, S., Hoffman, M. D., and Wilson, A. G. What are Bayesian neural network posteriors really like? In *International Conference on Machine Learning (ICML)*, 2021.

Khan, M. E. and Lin, W. Conjugate-computation variational inference: Converting variational inference in non-conjugate models to inferences in conjugate models. In *International Conference on Artificial Intelligence and Statistics (AISTATS)*, 2017.

Khan, M. E. and Rue, H. The Bayesian learning rule. arXiv:2107.04562, 2021.

Khan, M. E., Nielsen, D., Tangkaratt, V., Lin, W., Gal, Y., and Srivastava, A. Fast and scalable Bayesian deep learning by weight-perturbation in Adam. In *International Conference on Machine Learning (ICML)*, 2018.

Kingma, D. P. and Ba, J. Adam: A method for stochastic optimization. In *International Conference on Learning Representations (ICLR)*, 2015. arXiv:1412.6980.

Kingma, D. P., Salimans, T., and Welling, M. Variational dropout and the local reparameterization trick. In *Advances in Neural Information Processing Systems (NeurIPS)*, 2015.

Koh, P. W. and Liang, P. Understanding black-box predictions via influence functions. In *International Conference on Machine Learning (ICML)*, 2017.

Krizhevsky, A. Learning multiple layers of features from tiny images. Technical report, University of Toronto, 2009.

Lakshminarayanan, B., Pritzel, A., and Blundell, C. Simple and scalable predictive uncertainty estimation using deep ensembles. In *Advances in Neural Information Processing Systems (NeurIPS)*, 2017.

Le, Y. and Yang, X. S. Tiny ImageNet visual recognition challenge. Technical report, Stanford University, 2015.

Levesque, H., Davis, E., and Morgenstern, L. The winograd schema challenge. In *International Conference on the Principles of Knowledge Representation and Reasoning*, 2012.

Liang, S., Li, Y., and Srikant, R. Enhancing the reliability of out-of-distribution image detection in neural networks. In *ICLR*, 2018.

Lin, W., Khan, M. E., and Schmidt, M. Fast and simple natural-gradient variational inference with mixture of exponential-family approximations. In *International Conference on Machine Learning (ICML)*, 2019.

Lin, W., Schmidt, M., and Khan, M. E. Handling the positive-definite constraint in the Bayesian learning rule. In *International Conference on Machine Learning (ICML)*, 2020.

Liu, H., Li, Z., Hall, D., Liang, P., and Ma, T. Sophia: A scalable stochastic second-order optimizer for language model pre-training. In *International Conference on Learning Representations (ICLR)*, 2024.

Liu, Y., Ott, M., Goyal, N., Du, J., Joshi, M., Chen, D., Levy, O., Lewis, M., Zettlemoyer, L., and Stoyanov, V. RoBERTa: A robustly optimized BERT pretraining approach, 2019.

Loshchilov, I. and Hutter, F. Decoupled weight decay regularization. *arXiv:1711.05101*, 2017.

MacKay, D. J. C. A practical Bayesian framework for backpropagation networks. *Neural Comput.*, 4(3):448–472, 1992.

Maddox, W. J., Izmailov, P., Garipov, T., Vetrov, D. P., and Wilson, A. G. A simple baseline for Bayesian uncertainty in deep learning. In *Advances in Neural Information Processing Systems (NeurIPS)*, 2019.

Möllenhoff, T. and Khan, M. E. SAM as an optimal relaxation of Bayes. In *International Conference on Learning Representations (ICLR)*, 2023.

Netzer, Y., Wang, T., Coates, A., Bissacco, A., Wu, B., and Ng, A. Y. Reading digits in natural images with unsupervised feature learning. In *NIPS Workshop on Deep Learning and Unsupervised Feature Learning*, 2011.

Nickl, P., Xu, L., Tailor, D., Möllenhoff, T., and Khan, M. E. The memory perturbation equation: Understanding model's sensitivity to data. In *Advances in Neural Information Processing Systems (NeurIPS)*, 2023.

Nilsback, M.-E. and Zisserman, A. Automated flower classification over a large number of classes. In *Indian Conference on Computer Vision, Graphics and Image Processing*, 2008.

Noci, L., Roth, K., Bachmann, G., Nowozin, S., and Hofmann, T. Disentangling the roles of curation, data-augmentation and the prior in the cold posterior effect. In *Advances in Neural Information Processing Systems (NeurIPS)*, 2021.

Osawa, K., Swaroop, S., Jain, A., Eschenhagen, R., Turner, R. E., Yokota, R., and Khan, M. E. Practical deep learning with Bayesian principles. *Advances in Neural Information Processing Systems (NeurIPS)*, 2019.

Radford, A., Wu, J., Child, R., Luan, D., Amodei, D., Sutskever, I., et al. Language models are unsupervised multitask learners. *OpenAI blog*, 1(8):9, 2019.

Sato, M.-A. Online model selection based on the variational Bayes. *Neural computation*, 13(7):1649–1681, 2001.

Snoek, J., Ovadia, Y., Fertig, E., Lakshminarayanan, B., Nowozin, S., Sculley, D., Dillon, J. V., Ren, J., and Nado, Z. Can you trust your model's uncertainty? evaluating predictive uncertainty under dataset shift. In *Advances in Neural Information Processing Systems (NeurIPS)*, 2019.

Socher, R., Perelygin, A., Wu, J., Chuang, J., Manning, C. D., Ng, A., and Potts, C. Recursive deep models for semantic compositionality over a sentiment treebank. In *Conference on Empirical Methods in Natural Language Processing (EMNLP)*, 2013.

Srivastava, N., Hinton, G., Krizhevsky, A., Sutskever, I., and Salakhutdinov, R. Dropout: A simple way to prevent neural networks from overfitting. *Journal of Machine Learning Research*, 15(56):1929–1958, 2014.

Trippe, B. and Turner, R. Overpruning in variational Bayesian neural networks. In *Advances in Approximate Bayesian Inference*, 2017.

Vaswani, A., Shazeer, N., Parmar, N., Uszkoreit, J., Jones, L., Gomez, A. N., Kaiser, L., and Polosukhin, I. Attention is all you need. *Advances in Neural Information Processing Systems (NeurIPS)*, 2017.

Wang, A., Singh, A., Michael, J., Hill, F., Levy, O., and Bowman, S. GLUE: A multi-task benchmark and analysis platform for natural language understanding. In *EMNLP Workshop BlackboxNLP: Analyzing and Interpreting Neural Networks for NLP*, 2018.

Warstadt, A., Singh, A., and Bowman, S. R. Neural network acceptability judgments. *arXiv preprint arXiv:1805.12471*, 2018.

Welling, M. and Teh, Y. W. Bayesian learning via stochastic gradient Langevin dynamics. In *International Conference on Machine Learning (ICML)*, 2011.

Wen, Y., Vicol, P., Ba, J., Tran, D., and Grosse, R. B. Flipout: Efficient pseudo-independent weight perturbations on mini-batches. In *International Conference on Learning Representations (ICLR)*, 2018.

Wenzel, F., Roth, K., Veeling, B. S., Swiatkowski, J., Tran, L., Mandt, S., Snoek, J., Salimans, T., Jenatton, R., and Nowozin, S. How good is the bayes posterior in deep neural networks really? In *International Conference on Machine Learning (ICML)*, 2020.

Williams, A., Nangia, N., and Bowman, S. A broad-coverage challenge corpus for sentence understanding through inference. In *Conference of the North American Chapter of the Association for Computational Linguistics: Human Language Technologies, Volume 1 (Long Papers)*, 2018.

Wilson, A. G., Izmailov, P., Hoffman, M. D., Gal, Y., Li, Y., Pradier, M. F., Vikram, S., Foong, A., Lotfi, S., and Farquhar, S. Evaluating approximate inference in Bayesian deep learning. In *Proceedings of the NeurIPS 2021 Competitions and Demonstrations Track*, 2022.

Yao, Z., Gholami, A., Shen, S., Mustafa, M., Keutzer, K., and Mahoney, M. W. AdaHessian: an adaptive second order optimizer for machine learning. In *AAAI Conference on Artificial Intelligence (AAAI)*, 2021.

Zhang, G., Sun, S., Duvenaud, D., and Grosse, R. Noisy natural gradient as variational inference. In *International Conference on Machine Learning (ICML)*, 2018.

A. Practical Guideline for Choosing IVON Hyperparameters

To facilitate the usage of IVON, we provide here some practical guidelines for choosing hyperparameters and refer to their notations from Algorithm 1.

Learning rate schedule α_t. For ResNets, the initial learning rate of IVON can be set to the same value that works well for SGD, or slightly larger. For Transformers, we have found larger learning rates to work well, such as 0.1 for finetuning RoBERTa (Liu et al., 2019), or 0.2 for pretraining GPT-2 (Radford et al., 2019) with 355M parameters. Typical learning rate schedules like linear decay or cosine annealing work well for IVON. We have found decaying the learning rate to 0 to work best for pretraining GPT-2, better than decaying it to the initial learning rate divided by 10 as suggested by Hoffmann et al. (2022).

Effective sample size λ. Setting this to the size of training dataset ($\lambda = N$) in Eq. (1) is a good starting point. This recovers the standard evidence lower bound objective for variational learning. Setting it smaller is equivalent to increased temperature and setting it higher to decreased temperature. In our experiments we mostly set $\lambda \approx N$, except for finetuning transformers on very small datasets where we notice larger λ can improve performance and stabilize the short training. As seen from line 8 in Alg. 1, the choice of λ directly influences the posterior variance and too small values may lead to a high variance and unstable training whereas too large values may lead to a collapsed posterior that offers little benefits.

Weight decay δ. For ResNets, the weight decay of IVON can be set to the same values that work well for SGD or Adam. For Transformers, we have found smaller values, such as 10^{-5}, which we use for finetuning, or 10^{-6}, which we use for pretraining, to work well for weight decay. Larger values are feasible when using a quadratic penalty biased to the initialization of the model for finetuning.

Gradient momentum β_1. Setting $\beta_1 = 0.9$ tends to work well, similar to SGD or Adam. This plays a similar role as the gradient momentum in other optimizers so we expect the good settings to be similar.

Hessian momentum β_2. The Hessian momentum needs to be set rather close to one, for example, $\beta_2 = 1 - 10^{-5}$ worked well in our experiments. The Hessian momentum in theory is given by $\beta_2 = 1 - \lambda^{-1} N \rho$, where ρ is the step-size of natural gradient descent. If β_2 is set too small, for example, 0.999 or 0.9999 the training can sometimes become unstable.

Hessian initialization h_0. Along with the effective sample size λ, the Hessian initialization h_0 controls the noise at initialization. Typically values between 0.01 and 1 work well in practice but also smaller values like 0.001 have shown good results. Large values of h_0 correspond to more concentrated and deterministic initial posterior and can help stabilizing the training, but this can lead to poorer results. It can be helpful to monitor the statistics of the Hessian vector $\mathbf{h}$ during training, to see whether a reasonable covariance is being learned.

Batch size, training epochs. Typical batch sizes and training epochs that work well for SGD and AdamW tend to also work well for IVON. For example, our GPT-2 results in Fig. 1(a) use the same batch size and number of epochs for IVON and AdamW. This said, we observe that longer training and larger batch size seems to benefit IVON more than SGD, possibly because this would further improve the Hessian estimate.

Clip radius ξ. When training transformers, element-wise gradient clipping can stabilize the training. A clip-radius of $\xi = 10^{-3}$ worked well in practice. When picking a smaller clip-radius, one often requires a larger learning rate.

B. Ablation Studies

B.1. Computational Efficiency of IVON

The computational budget required by IVON is similar to standard deep learning optimizers. To validate its efficiency empirically, we measure the run time and peak GPU memory usage for image classification experiments on CIFAR-10 with ResNet-20 (He et al., 2016a) with an identical setup except for the choice of optimizer. Table 6 shows that IVON has similar computational costs as SGD and AdamW. However, we find a slight overhead when training larger models like GPT-2 as shown in Fig. 1(a), potentially because of the additional sampling step and unoptimized implementation.

	Runtime (hrs)				Memory (GB)			
	AdamW	SGD	VOGN	IVON	AdamW	SGD	VOGN	IVON
ResNet-20	0.38	0.38	0.68	0.38	1.7	1.7	2.0	1.7
GPT-2 (125M)	15.0	-	-	18.5	21.8	-	-	23.2
GPT-2 (355M)	37.5	-	-	44.7	23.7	-	-	27.7

Table 6: Runtime and memory for CIFAR-10 classification results with ResNet-20 and pretraining GPT-2 on OpenWebText. IVON has a small overhead for larger models which might be due to the additional weight sampling and a not fully optimized implementation.

	Acc. ↑	NLL ↓	ECE ↓	Brier ↓	Mem ↓
SG	$88.81_{\pm 0.31}$	$0.464_{\pm 0.020}$	$0.070_{\pm 0.004}$	$0.180_{\pm 0.006}$	**363MB**
GGN	$92.37_{\pm 0.23}$	$0.226_{\pm 0.005}$	$\mathbf{0.008}_{\pm 0.001}$	$0.111_{\pm 0.003}$	645MB
Reparam.	$\mathbf{92.64}_{\pm 0.13}$	$\mathbf{0.219}_{\pm 0.005}$	$\mathbf{0.009}_{\pm 0.002}$	$\mathbf{0.107}_{\pm 0.002}$	**363MB**

Table 7: IVON's reparameterization-trick-based Hessian estimator has better accuracy and uncertainty than other Hessian estimators at low computational cost, here for ResNet-20 on CIFAR-10.

B.2. Comparison of Hessian estimators

IVON's efficiency is enabled by estimating $\mathbf{g}_h$ with the reparameterization-trick-based estimator in Eq. 3. Here, we compare this estimator to the two squared-gradient estimators discussed in the previous section: 1) the Squared Gradient (SG) estimator which uses the square of mini-batch gradients $\widehat{\mathbf{h}} \leftarrow \widehat{\mathbf{g}}^2$ used in Vprop and Vadam (Khan et al., 2018); 2) the Gauss-Newton (GN) estimator which uses per-sample squared gradients, $\widehat{\mathbf{h}} \leftarrow \frac{1}{|\mathbb{B}|} \sum_{i \in \mathbb{B}} \left[\nabla \ell_i(\boldsymbol{\theta} + \boldsymbol{\sigma}\boldsymbol{\epsilon})\right]^2$ used in VOGN (Osawa et al., 2019). One drawback of the GN estimator is that per-example gradients require significant overhead, since the backpropagation process of typical deep learning frameworks only computes an averaged mini-batch gradient $\widehat{\mathbf{g}}$.

Table 7 shows results for training ResNet-20 on CIFAR-10 with these estimators. We observe that the reparameterization estimator provides best performance. The squared gradient estimator is similarly efficient but underperforms, whereas Gauss-Newton incurs significant overhead in GPU memory and time usage without large benefits in test performance.

B.3. Hessian initialization

We perform an ablation over the Hessian initialization h_0 used in Alg. 1. The model is a ResNet-20 trained on CIFAR-10. The results are summarized in the following Table 8.

h_0	Acc. ↑	NLL ↓	ECE ↓	Brier ↓
0.001	$9.89_{\pm 00.24}$	$2.3027_{\pm 0.0001}$	$0.0033_{\pm 0.0024}$	$0.9000_{\pm 0.0000}$
0.002	$43.95_{\pm 31.24}$	$1.4919_{\pm 0.7403}$	$0.0495_{\pm 0.0410}$	$0.6328_{\pm 0.2440}$
0.005	$82.78_{\pm 00.50}$	$0.5612_{\pm 0.0093}$	$0.1098_{\pm 0.0024}$	$0.2660_{\pm 0.0049}$
0.01	$86.74_{\pm 00.15}$	$0.4477_{\pm 0.0056}$	$0.1019_{\pm 0.0006}$	$0.2108_{\pm 0.0028}$
0.02	$89.60_{\pm 00.35}$	$0.3598_{\pm 0.0082}$	$0.0871_{\pm 0.0032}$	$0.1690_{\pm 0.0034}$
0.05	$91.72_{\pm 00.09}$	$0.2777_{\pm 0.0035}$	$0.0604_{\pm 0.0030}$	$0.1318_{\pm 0.0015}$
0.1	$92.25_{\pm 00.17}$	$0.2419_{\pm 0.0026}$	$0.0388_{\pm 0.0031}$	$0.1174_{\pm 0.0017}$
0.2	$92.44_{\pm 00.18}$	$0.2243_{\pm 0.0043}$	$0.0186_{\pm 0.0012}$	$0.1106_{\pm 0.0020}$
0.5	$\mathbf{92.71}_{\pm 00.07}$	$\mathbf{0.2173}_{\pm 0.0045}$	$\mathbf{0.0066}_{\pm 0.0015}$	$\mathbf{0.1069}_{\pm 0.0012}$
1	$92.61_{\pm 00.08}$	$0.2329_{\pm 0.0042}$	$0.0154_{\pm 0.0017}$	$0.1111_{\pm 0.0011}$
2	$92.46_{\pm 00.23}$	$0.2411_{\pm 0.0074}$	$0.0251_{\pm 0.0032}$	$0.1125_{\pm 0.0025}$
5	$92.34_{\pm 00.29}$	$0.2613_{\pm 0.0151}$	$0.0331_{\pm 0.0036}$	$0.1167_{\pm 0.0050}$

Table 8: The initialization of the Hessian $\mathbf{h}$ in Alg. 1 can be important to achieve the best results.

		Acc. ↑	Top-5 Acc. ↑	NLL ↓	ECE ↓	Brier ↓
ResNet-20 (272k params)	AdamW	$90.04_{\pm 0.27}$	$99.62_{\pm 0.03}$	$0.589_{\pm 0.018}$	$0.074_{\pm 0.002}$	$0.170_{\pm 0.004}$
	AdaHessian	$91.46_{\pm 0.06}$	$99.71_{\pm 0.02}$	$0.477_{\pm 0.018}$	$0.061_{\pm 0.001}$	$0.144_{\pm 0.001}$
	SGD	$91.86_{\pm 0.14}$	$\mathbf{99.70}_{\pm 0.08}$	$0.288_{\pm 0.015}$	$0.040_{\pm 0.004}$	$0.126_{\pm 0.003}$
	IVON@mean	$92.53_{\pm 0.04}$	$\mathbf{99.77}_{\pm 0.05}$	$0.256_{\pm 0.005}$	$0.034_{\pm 0.001}$	$0.115_{\pm 0.001}$
	IVON	$\mathbf{92.71}_{\pm 0.07}$	$\mathbf{99.78}_{\pm 0.03}$	$\mathbf{0.219}_{\pm 0.002}$	$\mathbf{0.008}_{\pm 0.001}$	$\mathbf{0.108}_{\pm 0.001}$
DenseNet-121 (1M params)	AdamW	$92.41_{\pm 0.26}$	$\mathbf{99.72}_{\pm 0.04}$	$0.594_{\pm 0.022}$	$0.062_{\pm 0.002}$	$0.135_{\pm 0.005}$
	AdaHessian	$\mathbf{92.95}_{\pm 0.87}$	$\mathbf{99.72}_{\pm 0.14}$	$0.514_{\pm 0.028}$	$0.056_{\pm 0.006}$	$0.124_{\pm 0.014}$
	SGD	$92.54_{\pm 0.30}$	$99.62_{\pm 0.04}$	$0.328_{\pm 0.008}$	$0.050_{\pm 0.003}$	$0.123_{\pm 0.003}$
	IVON@mean	$\mathbf{93.31}_{\pm 0.31}$	$\mathbf{99.74}_{\pm 0.03}$	$0.282_{\pm 0.014}$	$0.042_{\pm 0.003}$	$0.110_{\pm 0.004}$
	IVON	$\mathbf{93.53}_{\pm 0.26}$	$\mathbf{99.78}_{\pm 0.04}$	$\mathbf{0.200}_{\pm 0.007}$	$\mathbf{0.009}_{\pm 0.001}$	$\mathbf{0.096}_{\pm 0.003}$
PreResNet-110 (deep, 4M params)	AdamW	$92.39_{\pm 0.27}$	$99.69_{\pm 0.05}$	$0.653_{\pm 0.024}$	$0.064_{\pm 0.003}$	$0.137_{\pm 0.005}$
	AdaHessian	$\mathbf{93.76}_{\pm 0.25}$	$\mathbf{99.78}_{\pm 0.03}$	$0.431_{\pm 0.021}$	$0.049_{\pm 0.002}$	$0.109_{\pm 0.004}$
	SGD	$93.70_{\pm 0.15}$	$99.66_{\pm 0.08}$	$0.298_{\pm 0.010}$	$0.045_{\pm 0.001}$	$0.107_{\pm 0.002}$
	IVON@mean	$\mathbf{93.99}_{\pm 0.08}$	$\mathbf{99.80}_{\pm 0.03}$	$0.259_{\pm 0.008}$	$0.042_{\pm 0.001}$	$0.100_{\pm 0.002}$
	IVON	$\mathbf{94.02}_{\pm 0.14}$	$\mathbf{99.84}_{\pm 0.03}$	$\mathbf{0.180}_{\pm 0.003}$	$\mathbf{0.010}_{\pm 0.001}$	$\mathbf{0.087}_{\pm 0.001}$
ResNet-18 (wide, 11M params)	AdamW	$92.40_{\pm 0.32}$	$99.69_{\pm 0.05}$	$0.676_{\pm 0.006}$	$0.064_{\pm 0.003}$	$0.137_{\pm 0.005}$
	AdaHessian	$88.66_{\pm 1.51}$	$99.38_{\pm 0.13}$	$0.569_{\pm 0.037}$	$0.081_{\pm 0.008}$	$0.190_{\pm 0.023}$
	SGD	$94.03_{\pm 0.14}$	$99.72_{\pm 0.03}$	$0.282_{\pm 0.009}$	$0.043_{\pm 0.002}$	$0.101_{\pm 0.003}$
	IVON@mean	$\mathbf{94.17}_{\pm 0.08}$	$\mathbf{99.78}_{\pm 0.04}$	$0.305_{\pm 0.007}$	$0.045_{\pm 0.001}$	$0.102_{\pm 0.002}$
	IVON	$\mathbf{94.32}_{\pm 0.13}$	$\mathbf{99.84}_{\pm 0.03}$	$\mathbf{0.175}_{\pm 0.002}$	$\mathbf{0.010}_{\pm 0.001}$	$\mathbf{0.084}_{\pm 0.001}$

Table 9: IVON results on CIFAR-10 compared with various baseline optimizers using convolutional networks with different widths and depths. IVON@mean denotes point estimate results evaluated at the mean of IVON posterior.

C. Experimental Details

C.1. Pretraining GPT-2 Models on OpenWebText

We pretrain GPT-2 models (Radford et al., 2019) on OpenWebText (Gokaslan & Cohen, 2019) for multiple epochs and around 49.2B tokens in total using a batch size of 480 which is achieved by gradient accumulation. We train on 8 NVIDIA A100 GPUs with 40GB GPU memory each for up to three days. We use 2,000 warmup steps, 100,000 training steps in total, and evaluate every 1,000 steps on a held-out set. Each validation step is shown in Fig. 1(a). The learning rate is decayed to 0, which we have found to work better than $1/10$-times the initial learning rate for both AdamW and IVON. This is recommended in prior work (Hoffmann et al., 2022). For IVON, we use an initial learning rate of 0.3 for the 125M parameter checkpoint, 0.2 for the 355M parameter checkpoint, and 0.15 for the 773M parameter checkpoint. Note, that we do not rescale by $\mathbf{h}_0$ and δ in this case, because element-wise clipping is used. We use $\beta_1 = 0.9$, $\beta_2 = 1 - 10^{-5}$, $h_0 = 0.001$ and a weight decay factor of 10^{-6}, as well as element-wise clipping of 10^{-3}. These hyperparameters were found by grid search on a smaller model and it is possible that better hyperparameter configurations exist. We train with a single MC sample.

For training GPT-2 with AdamW, we use an initial learning rate of $6 \cdot 10^{-4}$, $\beta_1 = 0.9$, $\beta_2 = 0.95$ and a weight decay of 0.1. This follows the hyperparameters used in prior works (Liu et al., 2024). We follow the implementation in `https://github.com/karpathy/nanoGPT/`, which uses GeLU activations (Hendrycks & Gimpel, 2016) and does not use dropout (Srivastava et al., 2014) and biases during pretraining.

C.2. Training with IVON for Image Classification

We train a ResNet-50 (≈ 25.6 million parameters) (He et al., 2016a) with filter response normalization on the ImageNet dataset (≈ 1.2 million examples with 1000 classes) (Deng et al., 2009). Training for 200 epochs takes around 30 hours on 8 A100 GPUs for all methods. Our distributed implementation of IVON uses different random perturbations on each accelerator. IVON's initial learning rate is 2.5, we set $\beta_1 = 0.9$, $\beta_2 = 1 - 5 \cdot 10^{-6}$, $\delta = 5 \cdot 10^{-5}$, $h_0 = 0.05$ and $\lambda = N = 1281167$. No clipping is used and we train with a single MC sample. SGD uses a learning rate of 0.5 with same momentum $\beta_1 = 0.9$ and weight-decay $\delta = 5 \cdot 10^{-5}$. AdamW uses $\beta_1 = 0.9$, $\beta_2 = 0.999$, learning rate 0.001 and

weight-decay 0.1. The damping parameter in AdamW is set to the PyTorch default value $\varepsilon = 10^{-8}$, and larger values could potentially bring the AdamW performance closer to SGD. All methods anneal the learning rate to zero with a cosine learning rate schedule after a linear warmup phase over 5 epochs.

Here we also include additional image classification results using also deeper DenseNet-121 (Huang et al., 2017) and ResNet-20 in addition to ResNet-18 and PreResNet-110 (He et al., 2016b) on CIFAR-10 and the previously reported CIFAR-100 (Krizhevsky, 2009) and TinyImageNet (Le & Yang, 2015). The results are summarized in Tables 9, 10 and 11. We also compare to AdaHessian (Yao et al., 2021). We find that IVON improves over other optimizers in terms of both accuracy and uncertainty, across all datasets and all metrics. Finally, IVON does not overfit on smaller datasets.

For the experiments on CIFAR and TinyImageNet in Tables 1 and 9 to 11, the hyperparameters of all methods were tuned only for the ResNet-20 on CIFAR-10, and kept fixed across the other models and datasets. For SGD the learning rate $\alpha = 0.1$ was the largest stable learning rate across all models and datasets and gave the best results. AdaHessian uses $\alpha = 0.05$. It was not stable across all datasets when using the same learning rate as SGD as recommended by Yao et al. (2021). AdamW uses learning rate $\alpha = 0.002$, except for the PreResNet-110 on TinyImageNet, where we reran with $\alpha = 0.0005$ to get it to converge. We set $\beta_2 = 0.999$ in AdamW. IVON uses $\alpha = 0.2$, $\beta_2 = 1 - 10^{-5}$, $\lambda = N$ and $h_0 = 0.5$. All methods use gradient momentum $\beta_1 = 0.9$. We ran all optimizers for 200 epochs with batch-size 50. The learning rate was warmed up for 5 epochs using a linear schedule, and then decayed using a cosine learning rate annealing. The weight-decay is set to $\delta = 0.0002$ for all algorithms, datasets and models.

C.3. In-domain and OOD Comparison to Bayesian Deep Learning Methods

We train all ResNet-20 models with 200 epochs and batch size 50. Weight decay is set to 0.0002. Apart from SWAG, which requires custom scheduling, all other methods use 5 warm-up epochs followed by a cosine annealing learning rate schedule that decays to zero. We do 5 runs with different random seeds and report the average results and their standard deviations in the tables.

For the uncertainty estimation metrics used in in-domain and distributional shift experiments, we follow Snoek et al. (2019)

		Acc. ↑	Top-5 Acc. ↑	NLL ↓	ECE ↓	Brier ↓
ResNet-20 (272k params)	AdamW	$60.76_{\pm 0.47}$	$86.81_{\pm 0.48}$	$1.931_{\pm 0.044}$	$0.202_{\pm 0.004}$	$0.580_{\pm 0.008}$
	AdaHessian	$64.19_{\pm 0.28}$	$88.68_{\pm 0.39}$	$1.612_{\pm 0.033}$	$0.167_{\pm 0.007}$	$0.521_{\pm 0.004}$
	SGD	$67.23_{\pm 0.35}$	$90.75_{\pm 0.11}$	$1.173_{\pm 0.021}$	$0.059_{\pm 0.008}$	$0.441_{\pm 0.005}$
	IVON@mean	$\mathbf{67.87}_{\pm 0.55}$	$90.95_{\pm 0.10}$	$1.168_{\pm 0.012}$	$0.069_{\pm 0.007}$	$0.438_{\pm 0.005}$
	IVON	$\mathbf{68.28}_{\pm 0.50}$	$\mathbf{91.27}_{\pm 0.05}$	$\mathbf{1.113}_{\pm 0.010}$	$\mathbf{0.018}_{\pm 0.003}$	$\mathbf{0.425}_{\pm 0.005}$
DenseNet-121 (1M params)	AdamW	$65.47_{\pm 0.93}$	$88.74_{\pm 0.80}$	$2.967_{\pm 0.104}$	$0.264_{\pm 0.007}$	$0.587_{\pm 0.015}$
	AdaHessian	$71.02_{\pm 0.57}$	$92.00_{\pm 0.17}$	$2.379_{\pm 0.038}$	$0.222_{\pm 0.005}$	$0.494_{\pm 0.010}$
	SGD	$70.74_{\pm 0.49}$	$91.82_{\pm 0.10}$	$1.230_{\pm 0.012}$	$0.131_{\pm 0.004}$	$0.427_{\pm 0.006}$
	IVON@mean	$72.67_{\pm 0.43}$	$92.86_{\pm 0.14}$	$1.118_{\pm 0.017}$	$0.119_{\pm 0.002}$	$0.397_{\pm 0.005}$
	IVON	$\mathbf{73.68}_{\pm 0.37}$	$\mathbf{93.31}_{\pm 0.15}$	$\mathbf{0.940}_{\pm 0.012}$	$\mathbf{0.022}_{\pm 0.002}$	$\mathbf{0.361}_{\pm 0.004}$
PreResNet-110 (deep, 4M params)	AdamW	$65.88_{\pm 0.84}$	$88.34_{\pm 0.56}$	$2.893_{\pm 0.088}$	$0.258_{\pm 0.006}$	$0.578_{\pm 0.014}$
	AdaHessian	$72.43_{\pm 0.36}$	$91.92_{\pm 0.38}$	$1.844_{\pm 0.044}$	$0.194_{\pm 0.004}$	$0.452_{\pm 0.008}$
	SGD	$74.19_{\pm 0.11}$	$92.41_{\pm 0.14}$	$1.204_{\pm 0.012}$	$0.137_{\pm 0.002}$	$0.393_{\pm 0.004}$
	IVON@mean	$75.23_{\pm 0.23}$	$93.45_{\pm 0.16}$	$1.149_{\pm 0.010}$	$0.136_{\pm 0.002}$	$0.380_{\pm 0.003}$
	IVON	$\mathbf{75.81}_{\pm 0.18}$	$\mathbf{93.93}_{\pm 0.19}$	$\mathbf{0.884}_{\pm 0.007}$	$\mathbf{0.030}_{\pm 0.003}$	$\mathbf{0.336}_{\pm 0.001}$
ResNet-18 (wide, 11M params)	AdamW	$64.12_{\pm 0.43}$	$86.85_{\pm 0.51}$	$3.357_{\pm 0.071}$	$0.278_{\pm 0.005}$	$0.615_{\pm 0.008}$
	AdaHessian	$56.42_{\pm 6.22}$	$80.56_{\pm 4.81}$	$2.503_{\pm 0.261}$	$0.258_{\pm 0.014}$	$0.666_{\pm 0.071}$
	SGD	$74.46_{\pm 0.17}$	$92.66_{\pm 0.06}$	$1.083_{\pm 0.007}$	$0.113_{\pm 0.001}$	$0.376_{\pm 0.001}$
	IVON@mean	$74.51_{\pm 0.24}$	$92.74_{\pm 0.19}$	$1.284_{\pm 0.013}$	$0.152_{\pm 0.003}$	$0.399_{\pm 0.002}$
	IVON	$\mathbf{75.14}_{\pm 0.34}$	$\mathbf{93.30}_{\pm 0.19}$	$\mathbf{0.912}_{\pm 0.009}$	$\mathbf{0.021}_{\pm 0.003}$	$\mathbf{0.344}_{\pm 0.003}$

Table 10: IVON results on CIFAR-100 compared with various baseline optimizers using convolutional networks with different widths and depths. IVON @mean denotes point estimate results evaluated at the mean of IVON posterior.

		Acc. ↑	Top-5 Acc. ↑	NLL ↓	ECE ↓	Brier ↓
ResNet-20 (272k params)	AdamW	$46.62_{\pm 0.78}$	$72.71_{\pm 0.75}$	$2.387_{\pm 0.042}$	$0.121_{\pm 0.004}$	$0.692_{\pm 0.009}$
	AdaHessian	$50.06_{\pm 0.53}$	$76.09_{\pm 0.29}$	$2.120_{\pm 0.016}$	$0.084_{\pm 0.007}$	$0.642_{\pm 0.004}$
	SGD	$\mathbf{51.08}_{\pm 0.22}$	$\mathbf{77.17}_{\pm 0.25}$	$\mathbf{1.989}_{\pm 0.007}$	$\mathbf{0.020}_{\pm 0.003}$	$\mathbf{0.622}_{\pm 0.002}$
	IVON@mean	$\mathbf{50.71}_{\pm 0.38}$	$\mathbf{76.82}_{\pm 0.41}$	$2.014_{\pm 0.017}$	$\mathbf{0.020}_{\pm 0.006}$	$\mathbf{0.629}_{\pm 0.005}$
	IVON	$\mathbf{50.85}_{\pm 0.42}$	$\mathbf{76.92}_{\pm 0.37}$	$2.017_{\pm 0.016}$	$0.060_{\pm 0.005}$	$0.632_{\pm 0.004}$
DenseNet-121 (1M params)	AdamW	$50.01_{\pm 0.28}$	$74.76_{\pm 0.32}$	$5.515_{\pm 0.112}$	$0.385_{\pm 0.003}$	$0.851_{\pm 0.004}$
	AdaHessian	$43.66_{\pm 10.76}$	$69.86_{\pm 9.69}$	$3.142_{\pm 0.320}$	$0.189_{\pm 0.150}$	$0.772_{\pm 0.044}$
	SGD	$56.57_{\pm 1.00}$	$80.46_{\pm 0.81}$	$1.913_{\pm 0.056}$	$0.126_{\pm 0.008}$	$0.585_{\pm 0.012}$
	IVON@mean	$\mathbf{58.47}_{\pm 0.10}$	$\mathbf{82.58}_{\pm 0.23}$	$1.675_{\pm 0.008}$	$0.046_{\pm 0.004}$	$\mathbf{0.542}_{\pm 0.003}$
	IVON	$\mathbf{58.90}_{\pm 0.34}$	$\mathbf{82.69}_{\pm 0.35}$	$\mathbf{1.644}_{\pm 0.012}$	$\mathbf{0.035}_{\pm 0.002}$	$\mathbf{0.536}_{\pm 0.003}$
PreResNet-110 (deep, 4M params)	AdamW	$50.65_{\pm 0.0^*}$	$74.94_{\pm 0.0^*}$	$4.487_{\pm 0.0^*}$	$0.357_{\pm 0.0^*}$	$0.812_{\pm 0.0^*}$
	AdaHessian	$55.03_{\pm 0.53}$	$78.49_{\pm 0.34}$	$2.971_{\pm 0.064}$	$0.272_{\pm 0.005}$	$0.690_{\pm 0.008}$
	SGD	$59.39_{\pm 0.50}$	$81.34_{\pm 0.30}$	$2.040_{\pm 0.040}$	$0.176_{\pm 0.006}$	$0.577_{\pm 0.007}$
	IVON@mean	$\mathbf{60.85}_{\pm 0.39}$	$\mathbf{83.89}_{\pm 0.14}$	$1.584_{\pm 0.009}$	$0.053_{\pm 0.002}$	$\mathbf{0.514}_{\pm 0.003}$
	IVON	$\mathbf{61.25}_{\pm 0.48}$	$\mathbf{84.13}_{\pm 0.17}$	$\mathbf{1.550}_{\pm 0.009}$	$\mathbf{0.049}_{\pm 0.002}$	$\mathbf{0.511}_{\pm 0.003}$
ResNet-18 (wide, 11M params)	AdamW	$47.33_{\pm 0.90}$	$71.54_{\pm 0.95}$	$6.823_{\pm 0.235}$	$0.421_{\pm 0.008}$	$0.913_{\pm 0.018}$
	AdaHessian	$51.80_{\pm 0.29}$	$75.01_{\pm 0.10}$	$3.416_{\pm 0.028}$	$0.304_{\pm 0.002}$	$0.748_{\pm 0.005}$
	SGD	$61.39_{\pm 0.18}$	$82.30_{\pm 0.22}$	$1.811_{\pm 0.010}$	$0.138_{\pm 0.002}$	$0.536_{\pm 0.002}$
	IVON@mean	$\mathbf{62.41}_{\pm 0.15}$	$\mathbf{83.77}_{\pm 0.18}$	$1.776_{\pm 0.018}$	$0.150_{\pm 0.005}$	$0.532_{\pm 0.002}$
	IVON	$\mathbf{62.68}_{\pm 0.16}$	$\mathbf{84.12}_{\pm 0.24}$	$\mathbf{1.528}_{\pm 0.010}$	$\mathbf{0.019}_{\pm 0.004}$	$\mathbf{0.491}_{\pm 0.001}$

Table 11: IVON results on TinyImageNet compared with various baseline optimizers using convolutional networks with different widths and depths. IVON @mean denotes point estimate results evaluated at the mean of IVON posterior. (*) AdamW only converged for one of the five random seeds for PreResNet-110.

and report three metrics: negative log-likelihood (NLL), expected calibration error (ECE), and Brier score. For the OOD experiments we used the same metrics as Liang et al. (2018), i.e. False Positive Rate (FPR), the share of misclassified OOD samples, at 95% TPR, detection error, which measures the probability of misclassifications for 95% TPR, Area Under the Receiver Operating Characteristic curve (AUROC), AUPR-in, and AUPR-out. Here, AUPR stands for Area under the Precision-Recall for the in-domain data (AUPR-in) or OOD data (AUPR-out), respectively.

The specific training hyperparameters for each method are:

- SGD and IVON use the same setting as in Section C.2, except that SGD also uses learning rate 0.2 which is stable for ResNet-20;
- VOGN uses the same hyperparameter setup as IVON;
- BBB uses learning rate 0.002. We set the same initial posterior as IVON and train BBB without using a cold posterior;
- Laplace uses the linearized last-layer Laplace implementation from Daxberger et al. (2021) and the prior precision is set to 10.0 corresponding to the same prior setup as other methods;
- MC dropout uses learning rate 0.2 and a fixed dropout rate of 0.05;
- For SWAG, we first do normal training with cosine annealing from lr 0.05 to 0.01 over 160 epochs, then do 40 SWAG epochs with constant learning rate 0.01 and maintain a rank 20 approximation of the SWAG posterior as is done in (Maddox et al., 2019).

We use 64 posterior samples for IVON, BBB, Laplace, SWAG and VOGN. For MC dropout, we only draw 32 samples for all experiments as we observe no improvement when drawing 64 samples.

	MNLI-m	QNLI	QQP	RTE	SST2	MRPC	CoLA	STS-B
Metric	Acc.	Acc.	Acc.	Acc.	Acc.	Acc / F1	Spearman	MCC
#Train	393k	105k	364k	2.5k	67k	3.7k	8.5k	7k
#Validation	9.8k	5.5k	40.4k	277	872	408	1k	1.5k

Table 12: Dataset sizes of individual GLUE tasks used in this paper and the used evaluation metrics.

C.4. Finetuning on GLUE

GLUE (Wang et al., 2018) is a multi-task benchmark consisting of in total 9 diverse tasks which capture classification and regression problems. We use all tasks but WNLI (Levesque et al., 2012) following previous work (Devlin et al., 2019). Namely, we use: CoLA (Warstadt et al., 2018), MNLI (Williams et al., 2018), MRPC (Dolan & Brockett, 2005), QNLI (Wang et al., 2018), QQP, RTE, SST2 (Socher et al., 2013), and STS-B (Cer et al., 2017).

For IVON, we use the same hyperparameters for the two models used in our experiments: RoBERTa and DeBERTav3 shown in Sec. 4.3.1. We use an initial learning rate of 0.1 or 0.2 which is decayed to 0.0 using cosine decay. We set $\beta_1 = 0.9$, $\beta_2 = 1 - 10^{-5}$, $h_0 = 1.0$, a weight decay factor of 10^{-5}, and also use element-wise clipping of 10^{-3}. Furthermore, we use 500 warmup steps.

For RoBERTa with AdamW, we use the hyperparameters reported in (Liu et al., 2019, Table 10). Namely, we sweep learning rates over $\{10^{-5}, 2 \cdot 10^{-5}, 3 \cdot 10^{-5}\}$. We use a weight decay of 0.1, $\beta_1 = 0.9$, and $\beta_2 = 0.98$.

For DeBERTAv3 with AdamW we use the hyperparameters as reported in (He et al., 2023, Table 11) but were unable to sweep all possible combinations that are listed due to the high computational demand. Therefore, we fix the number of warmup steps to 500 and the batch size to 32. Also, we do not use last layer dropout. We sweep learning rates over $\{5 \cdot 10^{-6}, 8 \cdot 10^{-6}, 9 \cdot 10^{-6}, 10^{-5}\}$, use a weight decay of 0.1, $\beta_1 = 0.9$, and $\beta_2 = 0.999$.

We evaluate after each epoch and train for up to 10 epochs on every dataset but MRPC, where we allow 15 epochs. The batch size is always set to 32 for both AdamW and IVON.

C.5. Predicting Generalization and Understanding Models' Sensitivity to Data

We use the memory-perturbation equation (MPE) by Nickl et al. (2023). In their framework, prediction error and variances for a multi-output vector $\mathbf{f}_i(\boldsymbol{\theta}_t) \in \mathbb{R}^C$ (with C being the number of classes) at iteration t are obtained as follows,

$$\mathbf{e}_{it} = \mathcal{S}(\mathbf{f}_i(\boldsymbol{\theta}_t)) - \mathbf{y}_i, \qquad \mathbf{V}_{it} = \nabla \mathbf{f}_i(\boldsymbol{\theta}_t)^\top \text{diag}(\boldsymbol{\sigma}_t^2) \nabla \mathbf{f}_i(\boldsymbol{\theta}_t),$$

where $\mathcal{S}(\cdot)$ is the softmax function and $\nabla \mathbf{f}_i(\boldsymbol{\theta}_t) \in \mathbb{R}^{P \times C}$ is the Jacobian with P being the number of parameters.

For IVON, we set $\boldsymbol{\theta}_t = \mathbf{m}_t$ and use the posterior variance $\boldsymbol{\sigma}_t^2 = 1/\lambda(\mathbf{h}_t + \delta)$. For SGD and AdamW, we construct $\boldsymbol{\sigma}_t^2$ in ad-hoc ways. For SGD we use $\boldsymbol{\sigma}_t^2 = 1/N(\mathbf{1} + \delta)$. For AdamW we use $\boldsymbol{\sigma}_t^2 = 1/N(\sqrt{\mathbf{h}_t} + \delta)$, where $\mathbf{h}_t$ is the second moment vector that maintains a running-average of squared gradients.

For all data sensitivity experiments in the main paper we used the following hyperparameters to train a ResNet-50 on ImageNet for 100 epochs. IVON uses an initial learning rate of 3, $\beta_1 = 0.9$, $\beta_2 = 1 - 10^{-6}$, $h_0 = 0.008$, $\lambda = N$ and a weight decay of $\delta = 5 \cdot 10^{-5}$. h_0 was selected on a grid of $[0.008, 0.01, 0.05]$ to achieve a faithful estimate of generalization performance while keeping a competitive test accuracy. AdamW uses a learning rate of 0.001, $\beta_1 = 0.9$, $\beta_2 = 0.999$ and weight decay 0.1. Both methods use 5 warmup epochs after which the learning rate is decayed to 0 using cosine decay. The model trained with IVON has an accuracy of 75%, whereas the AdamW model has 74.7% accuracy.

D. Additional Results

D.1. IVON with Recurrent Neural Networks

We train a simple model based on Gated Recurrent Units (Cho et al., 2014) on three text classification datasets (CoLA, IMDB and AG News). The model consists of an embedding layer, two GRUs and a fully connected layer, for a total of 2 million parameters. We train the same model with SGD, AdamW and IVON. IVON results are evaluated both at the mean and at a Monte-Carlo approximation of the posterior using 64 samples. Results are reported in Table 13. IVON improves

		Acc. ↑	NLL ↓	ECE ↓	Brier ↓	AUROC ↑
CoLA	AdamW	$64.35_{\pm 0.27}$	$0.666_{\pm 0.026}$	$0.322_{\pm 0.026}$	$0.658_{\pm 0.048}$	$\mathbf{0.579}_{\pm 0.019}$
	SGD	$\mathbf{67.65}_{\pm 0.92}$	$0.631_{\pm 0.011}$	$0.060_{\pm 0.006}$	$0.448_{\pm 0.006}$	$0.548_{\pm 0.027}$
	IVON@mean	$\mathbf{68.54}_{\pm 0.00}$	$\mathbf{0.623}_{\pm 0.03}$	$\mathbf{0.030}_{\pm 0.005}$	$\mathbf{0.432}_{\pm 0.003}$	$0.509_{\pm 0.041}$
	IVON	$\mathbf{68.54}_{\pm 0.00}$	$\mathbf{0.623}_{\pm 0.03}$	$\mathbf{0.029}_{\pm 0.005}$	$\mathbf{0.432}_{\pm 0.003}$	$0.510_{\pm 0.041}$
IMDB	AdamW	$84.66_{\pm 0.46}$	$1.929_{\pm 0.344}$	$0.136_{\pm 0.007}$	$0.285_{\pm 0.011}$	$0.725_{\pm 0.013}$
	SGD	$85.06_{\pm 0.38}$	$\mathbf{0.468}_{\pm 0.013}$	$\mathbf{0.065}_{\pm 0.009}$	$0.233_{\pm 0.011}$	$0.764_{\pm 0.016}$
	IVON@mean	$\mathbf{89.55}_{\pm 0.20}$	$\mathbf{0.428}_{\pm 0.023}$	$\mathbf{0.061}_{\pm 0.003}$	$0.251_{\pm 0.023}$	$\mathbf{0.811}_{\pm 0.025}$
	IVON	$87.73_{\pm 0.96}$	$0.568_{\pm 0.119}$	$\mathbf{0.065}_{\pm 0.010}$	$\mathbf{0.199}_{\pm 0.018}$	$0.751_{\pm 0.031}$
AG News	AdamW	$90.65_{\pm 0.32}$	$0.985_{\pm 0.046}$	$0.408_{\pm 0.031}$	$0.171_{\pm 0.006}$	$0.826_{\pm 0.006}$
	SGD	$89.57_{\pm 0.40}$	$0.386_{\pm 0.009}$	$0.055_{\pm 0.004}$	$0.167_{\pm 0.005}$	$0.845_{\pm 0.004}$
	IVON@mean	$\mathbf{92.43}_{\pm 0.01}$	$\mathbf{0.233}_{\pm 0.003}$	$\mathbf{0.017}_{\pm 0.002}$	$\mathbf{0.118}_{\pm 0.001}$	$\mathbf{0.871}_{\pm 0.003}$
	IVON	$\mathbf{92.46}_{\pm 0.01}$	$\mathbf{0.231}_{\pm 0.002}$	$\mathbf{0.014}_{\pm 0.003}$	$\mathbf{0.117}_{\pm 0.001}$	$\mathbf{0.871}_{\pm 0.002}$

Table 13: IVON results on NLP classification datasets compared with to SGD and AdamW. IVON@mean denotes point estimate results evaluated at the mean of IVON posterior.

both accuracy and uncertainty compared to the baselines. The chosen model can easily overfit the presented datasets, achieving close to 100% accuracy on the training set. Therefore, extra care is required when choosing the hyperparameters for AdamW and, especially, SGD. However, we find it easier to tune IVON for satisfactory results both in terms of accuracy and uncertainty.

D.2. Robustness to Distribution Shift

Having trained and evaluated various models on CIFAR-10 in the in-domain scenario, here we conduct distributional shift experiments, where we use the previously trained networks to directly classify CIFAR-10 test set images corrupted with artificial perturbations. For this we use the CIFAR-10-C (Hendrycks & Dietterich, 2019) dataset which collects a range of common image distortions and artifacts, each with 5 severity levels. The results are grouped by severity level and summarized in Fig. 7 on the next page.

In general, the performance of all models decrease with increasing severity, as the classification task is getting harder. We observe that IVON keeps the best performance for low severity levels. For high severity levels, IVON is notably outperformed by SWAG. Despite this, IVON in general is still comparable to BDL baselines for high severity cases. And as an optimizer, it remains a better choice over the standard SGD training.

D.3. NeurIPS 2021 Approximate Inference Competition

An earlier version of IVON won the first place[1] in both the light and extended track of the NeurIPS 2021 Competition on Approximate Inference in Bayesian Deep Learning (Wilson et al., 2022). The earlier version included an additional heuristic damping to $\widehat{\mathbf{h}}$ in line 3 of Alg. 1 and the weight-decay was added in line 4 rather than in lines 5 and 6. We found the damping term to be unnecessary when using a proper Hessian initialization h_0 and momentum β_2 and therefore removed it, making IVON easier to tune. The three highest scoring submissions to the competition are summarized in Table 14. First place is Multi-IVON (using the earlier version of IVON), which is a mixture-of-Gaussian ensemble (with uniform weights) as described in the experiments section on uncertainty estimation in the main paper. The second place solution (Multi-SWAG) uses multiple runs of SWAG to construct a mixture-of-Gaussian approximation (Izmailov et al., 2021) with SGLD (Welling & Teh, 2011) as a base optimizer. Third place was obtained by a deep ensembling method called sequential anchored ensembles (SAE) (Delaunoy & Louppe, 2021). In Table 14, 'Agree' denotes predictive agreement with a ground-truth Bayesian posterior obtained by running Hamiltonian Monte-Carlo method on hundreds of TPUs. TVD denotes the total variation distance and W_2 the Wasserstein-2 distance between this ground-truth predictive posterior and the approximate posterior. We refer to Wilson et al. (2022) for more details.

[1] For the official results, see https://izmailovpavel.github.io/neurips_bdl_competition.

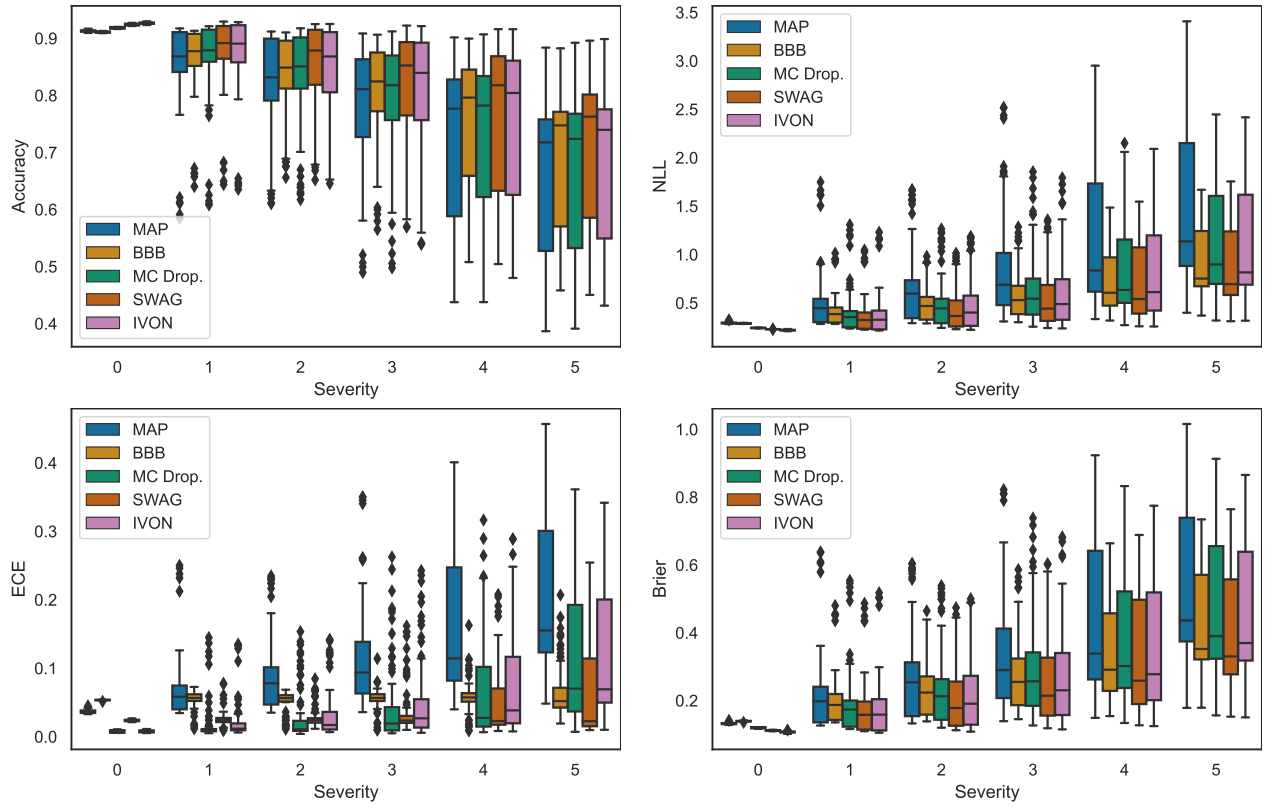

Figure 7: Distributional shift results on CIFAR-10-C with various degree of severities. Severity 0 corresponds to the in-domain case.

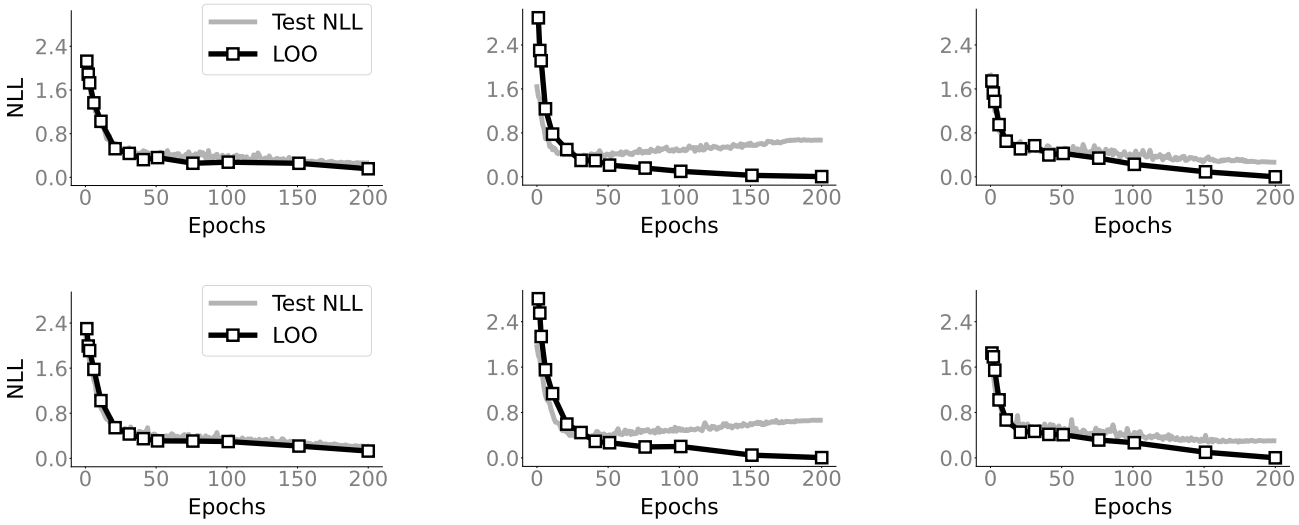

Figure 8: We predict test NLL using LOO estimation during training of two models on CIFAR10. From top to bottom the models are: ResNet–18 and PreResNet–110. IVON (first column) allows us to faithfully predict generalization, while the heuristic LOO estimates with AdamW (second column) and SGD (third column) work less well.

Rank	Method	CIFAR-10		MedMNIST		UCI
		Agree ↑	TVD ↓	Agree ↑	TVD ↓	W_2 ↓
1	Multi-IVON†	**78.7%**	**0.198**	88.4%	0.099	**0.094**
2	Multi-SWAG	77.8%	0.219	**89.0%**	**0.098**	0.166
3	SAE	77.3%	0.210	87.5%	0.107	0.116
	Multi-IVON (Alg. 1)	78.2%	0.204	89.1%	0.097	0.075

Table 14: An earlier version of IVON (denoted by †) won the NeurIPS 2021 competition on approximate inference in Bayesian deep learning (Wilson et al., 2022). The second best method used a combination of SWAG and SGLD. Third place was a Sequential Anchored Ensemble (SAE). In the last row of the table we also report results achieved with Alg. 1 which performs similarly well as the previous version of IVON.

D.4. Predicting Generalization

In Fig. 8, we conduct additional experiments with ResNet-18 and PreResNet-10 on the CIFAR-10 dataset. We estimate generalization performance during training using the LOO criterion described in App. C.5. The accuracy of IVON is similar to the SGD baseline. IVON however results in a more faithful estimate of the generalization performance in comparison to AdamW and SGD. We evaluate the sensitivity of the models to data perturbation as described in App. C.5 with the difference that we compute the sensitivities as $\mathbf{e}_i \mathbf{v}_i$, where $\mathbf{v}_i$ are the diagonal elements of $\mathbf{V}_i$ and $\mathbf{v}_i \mathbf{e}_i$ is an element-wise product. For training the models, we use the same hyperparameters as in the image classification experiments. The exception is the Hessian initialization h_0. We do a grid search over the values $[0.01, 0.05, 0.1, 0.5]$. We select the value that results in a faithful estimate of the generalization performance while keeping a competitive test accuracy. The Hessian initialization is set to $h_0 = 0.1$ for both models. The test accuracies are 93.68% for ResNet–18 and 93.52% for PreResNet–110 with predictions at the mean of the variational posterior.